The Effect of Moisture on Electrical Resistivity of

MWCNT Reinforced Epoxy Nanocomposites

Sima Nabavizadeh R.

A Thesis

in

The Department

of

Mechanical and Industrial Engineering

Presented in Partial Fulfillment of the Requirements

For the Degree of Master of Applied Science in Mechanical Engineering at

Concordia University

Montreal, Quebec, Canada

April 2015

This is to certify that the thesis prepared

By: Sima Nabavizadeh R.

Entitled: The Effect of Moisture on Electrical Resistivity of CNT Reinforced Epoxy Nanocomposites

and submitted in partial fulfillment of the requirements for the degree of

Master of Applied Science in Mechanical Engineering

Complies with the regulations of the university and meets the accepted standards with respect to originality and quality.

Signed by the final examining committee:

_____ Chair

_____ Examiner

_____ Examiner

_____ Supervisor

_____

Approved by   Chair of Department or Graduate Program Director

_____

_____   Dean of Faculty

ABSTRACT

The Effect of Moisture on the Electrical Conductivity of

MWCNT Reinforced Epoxy Nanocomposites

S. Nabavizadeh R.

Epoxy nanocomposites reinforced with carbon nanotubes have found their path through a wide range of applications in aerospace, automotive, and electronics packaging industries. This is due to the superior properties provided by carbon nanotubes such as enhancing mechanical strength and chemical resistance as well as thermal and electrical conductivity. However, epoxy composites have proved to be vulnerable to different environmental conditions such as humidity and temperature, and the role of carbon nanotubes in leading the extent of changes of their properties have been a subject of research in several studies. This research brought into focus the electrical properties of multi-walled carbon nanotube (MWCNT) reinforced epoxy nanocomposites exposed to humid environments. For this purpose, different concentrations of multi-walled carbon nanotubes were added to epoxy, and a wide range of conductivities were obtained. The nanocomposite was immersed in water, and its water uptake, alongside the changes in thickness and electrical resistivity were measured and analyzed. The water saturation level, regardless of the type and content of MWCNT or the temperature, remained unchanged. The diffusivity in a constant temperature was influenced by two factors of MWCNT attraction and MWCNT crowd. The electrical resistivity of the polymer increased with water uptake, and samples with higher MWCNT content showed less sensitivity to water absorption. Changes in the electrical resistivity were explained through a resistivity model. The increase in electrical resistivity was significantly higher with a faster swelling. This conclusion resulted from a comparative experiment conducted on MWCNT reinforced silicone rubber nanocomposite immersed in engine oil. Finally, desorption

behaviour of the epoxy nanocomposites was investigated. It was found that weight gain is recoverable at an elevated temperature, while a constant increase in electrical resistivity resides in the nanocomposite.

Acknowledgment

I would like to express my deepest gratitude to my supervisor, Dr. S.V. Hoa, whose continuous guidance and support encouraged me throughout the entire MASc thesis program. This thesis would not have been possible without him.

I am grateful to Dr. Rosca for his kind assistance and support, which facilitated the procedure of the project for me.

I would like to thank Dr. Ali Naghashpour, whose extremely helpful guidance and suggestions accompanied me throughout this path.

It was an honour for me to work and study alongside the members of CONCOM research group of Dr. Hoa.

And last but not least, I am indebted to my parents for their unconditional support and inspiration throughout my life, which led me to where I am right now. I am also thankful to my life partner, my brothers, my friends, and all those who were next to me and supported me kindly.

Dedication

I dedicate this thesis to my beloved life partner,

Bardia Dejam

Table of Contents

List of Figures

List of Tables

Nomenclature

Carbon Nanotube (CNT)

Multi-Walled Carbon Nanotube (MWCNT)

Single-Walled Carbon Nanotube (SWCNT)

Double-Walled Carbon Nanotube (DWCNT)

Cup-Stacked Carbon Nanotube (CSCNT)

Scanning Electron Microscopy (SEM)

Differential Scanning Calorimetry (DSC)

Chemical Vapor Deposition (CVD)

Electrically Conductive Adhesives (ECA)

Nuclear Magnetic Resonance (NMR)

Diglycidyl Ether of Bisphenol F (DGEBF)

Diethyltoluenediamine (DETDA)

Polydimethylsiloxane (PDMS)

1 Introduction, Literature Review, Problem Statement, and Objective

1.1 Introduction

Epoxy composites are light-weight materials offering superior properties such as high strength and stiffness and good chemical resistance. They have a wide range of applications in engineering structures such as automobiles and aircrafts. The addition of carbon nanotubes as multifunctional materials to epoxies, further expands their applicability. CNTs are nanoscale particles with large aspect ratios (length to diameter), and provide exceptional electrical and thermal conductivity, alongside reinforcing the mechanical performance of epoxies. Epoxy composites reinforced with carbon nanotubes, depending on the structure and the content of CNT, can obtain an extent of electrical conductivity, and have the potential to be used in electronics industries, as well as sensors for structural health monitoring techniques. However, one drawback in utilizing these materials is that, due to their hydrophilic characteristics, epoxies tend to absorb water in humid environments. The transport of water into the material alters the functionality of carbon nanotubes and affects the inherent and acquired properties of epoxies. That is to say, the electrical properties of the nanocomposite will be subject to change.

This chapter focuses on the introduction of epoxy composites and carbon nanotubes, their synthesis, individual and combined properties and applications, as well as their advantages and disadvantages. The studies conducted by other researchers on the mechanism of water absorption in the epoxy and its roles in altering mechanical, electrical, and physical properties of neat and

CNT reinforced epoxy composite are explained and summarized. The gaps in this field of research are defined, the objective of the thesis is specified, and finally, the contents of each chapter are mentioned.

1.2   Literature Review

1.2.1   Epoxy

Epoxy is a thermoset resin known as one of the most commonly used matrices in advanced structural composite materials and for a variety of demanding applications and manufacturing industries [1,2]. Its first commercial performance appeared around 1947 [3], and there have been tremendous advancements in its technology since then. Currently, superior thermal and mechanical properties, chemical and corrosion resistance, and electrical insulation, alongside satisfactory processing characteristics such as good mold flow, fast extrusion, and easy injection molding prompt epoxies to be one of the leader structural materials in aerospace, automobile, and civil industries [1,3,4].

Epoxy composites offer strong adhesion with reinforcements and also with the surface of other materials [1]. Epoxies meet dominant factors of stiffness, strength, and durability in choosing an adhesive. As structural adhesives, they provide properties that are worth replacing mechanical connections such as bolts, metallic fasteners, and metal soldering or welding. The advantages of Epoxies over metals include being light-weight, having integrity through the whole surface, ability of adhesion to all kinds of materials, and excellent cohesion, i.e. bulk adhesion.

Epoxy molding compounds are increasingly used in electronics and microelectronics packaging industry. Due to their low material and manufacturing costs, and high productivity and quality, they are used as encapsulants, circuit boards, and adhesives [5,6].

The first time that epoxies were found to have favourable adhesive-bonding properties, was in 1944 by Preiswerk and Gams [7]. They realized that Epoxies were "the first cast-in-place adhesives featuring a versatile chemical functionality and a remarkably low shrinkage on curing" [3] which resulted in low inner stresses. Lewis and Saxon [8] studied the adhesive joint strength of Epon 828 (diglycidyl ether of bisphenol A) cured with 10 phr of diethylenetriamine, and found the adhesion tensile strength below glass transition temperature to be around 7000-8000 psi. They also showed that the strength of the adhesive joints depends on the rheological state of the adhesive, and rubbery systems showed lower moduli, lap shear and tensile strengths, whereas glassy polymers exhibited higher moduli and adhesive-joint strengths [8].

1.2.1.1 Molecular Structure and Synthesis

Epoxy is a name given to a group of polymeric materials with Epoxide groups. Epoxide group is the part that provides α- or 1,2-epoxide or Glycidyl functional groups, consisting of an oxygen atom bridge connected to two connected Carbon atoms (Figure 1-1)[1]. This functional group is also the site of the cross-linking reaction. Diglycidyl ether of bisphenol A (DGEBA) is a common class of epoxy resins, which is formed from the reaction of two moles of epichlorohydrin and one mole of bisphenol A [1]. Figure 1-2 shows a 3-dimensional model of DGEBA molecular structure. Diglycidyl ether of bisphenol F (Figure 1-3), TGDDM, and TGMDA are other common epoxy resins [1].
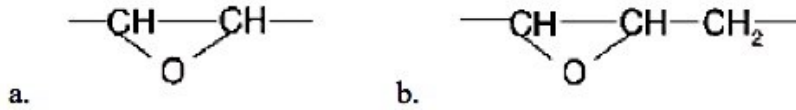
Figure 1-1 a) Epoxide group, b) Glycidyl group [1]
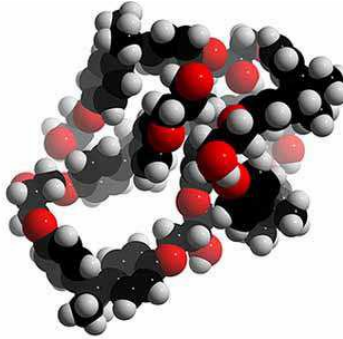
Figure 1-2 3-D Molecular structure of diglycidyl ether of bisphenol A (DGEBA) [9]
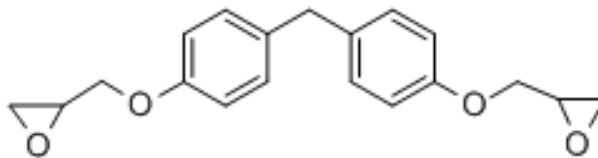
Figure 1-3 Molecular structure of diglycidyl ether of bisphenol F [10]

1.2.1.2   Curing

Epoxies are versatile in processing. During the curing process, no toxic gases are expelled, and the cured product has reduced stresses and low shrinkage. The physical properties of the final product can be enhanced by controlling the curing temperature and the degree of crosslinking [3]. The overall properties also depend on both the nature of the epoxy and the curing system [1]. Amines, anhydrides, and tertiary amines are common curing agents for epoxies. Amine molecules have active hydrogen atoms connected to their nitrogen atoms. This hydrogen separates from the nitrogen, reacts with the oxygen in the epoxide ring, and together they form a hydroxyl (O-H) group. The terminal carbon also reacts with the nitrogen and this way, two molecules form one molecule. This explains the procedure of cross-linking. All active hydrogen atoms connected to

nitrogen in primary amines (RNH$_2$) and secondary amines (RNH) can react with oxygen atoms in epoxide groups, and they define the number of cross-links in the polymer [1,11].

Depending on the type of epoxy, different curing temperatures from ambient to up to 200°C are required in order to achieve a complete polymerization, and hence, optimum mechanical, chemical and heat resistance.

1.2.2   Carbon Nanotubes

With emerging availability of nanoscale materials such as carbon nanotubes, flakes, fibers, plates, spheres, and particles, along with the growing technology at this scale, nano-engineered multi-functional materials hold the future key to the reinforcement of super advanced composites [12,13].

Carbon nanotubes, in particular, due to their high aspect ratios and specific surface area, the very appealing physical and mechanical properties, including high specific stiffness and strength and high elastic modulus, and also remarkable thermal and electrical conductivity, have demonstrated a great potential for a wide range of structural, functional, and sensing applications. [12,14-22]

Carbon nanotubes (CNTs) are fullerene or spheroidal cage-like structures with diameters of 1 to 20 nm, lengths of 0.5 to more than 10 μm, and aspect ratios of 30 to 300 [14,19,23,24]. The fullerene spheroidal structure was discovered for the first time by Smalley and co-workers in mid 1980s, which led to the synthesis of carbon nanotubes by Iijima in 1991 [15]. Carbon nanotubes are rolled graphite sheets; 2-D sheets of carbon atoms with hexagonal arrangements, in a way that each carbon atom is connected to three other carbon atoms. Graphite sheets roll into different forms of nanotubes depending on their chirality angle. If the angle is zero, the circumferential carbon

atoms form a zigzag structure, and if it is 30 degrees, the arrangement is called armchair (Figure 1-4). This chirality can affect the electrical properties of the CNT [14,15].
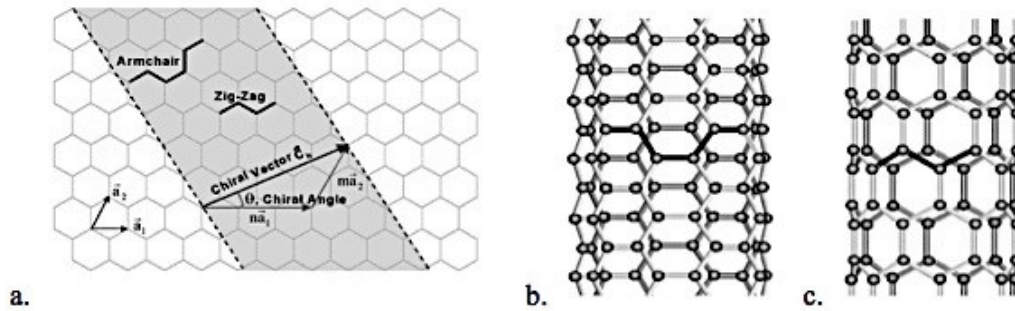
Figure 1-4 a) Schematic diagram of the twisting of the graphite sheet b) armchair c) zigzag nanotube structure [15]

Numerous studies have been conducted on the physical and mechanical properties of CNTs. The density of Single-wall CNT is 1.22-1.40 g/cm^3, which is almost half the density of aluminum. The elastic modulus of SWCNT is 1 TPa, similar to diamond, and its tensile strength is over 150 GPa, which exhibits a strength higher than that of high-strength steel [14,15]. According to Iijima et al. [15], carbon nanotubes are remarkably resilient, and can bend reversibly up to 110 degrees [15]. Their fracture strain is between 10 to 30%, while carbon fibers only survive 0.1-2% [15]. CNTs have superior thermal and electrical properties. The thermal conductivity of SWCNT is 6000 W/mK at room temperature, higher than 3320 W/mK for diamond. CNTs are stable up to 2800 °C in vacuum and 750 °C in air, whereas Metal wires in microchips melt at 600-1000 °C [15]. Copper wires burn out at the current density of 1x10^6 (amp/cm^2), while electrical current carrying capability of CNTs is about 1x10^9 (amp/cm^2), three orders of magnitude higher [13,15]. OH-functionalized CNTs, due to their polarity, attach other polar molecules like water on their surface [14].

CNTs have stimulated interest in a wide range of applications. Bu et al. [16] showed that SWCNTs were used as pressure sensors, with a high piezoresistive gauge factor of 210, while MWCNTs

were utilized for strain sensing applications [16]. Matthias et al. [17] also used CNTs to solve the concern of reliable interconnects in electronic packaging [17]. Jiang and coworkers [18] incorporated MWCNTs to make films with thousands of well-aligned parallel CNTs as interconnect materials in electronic and photonic devices [18]. Ling et al. [22] also exploited the high surface area to aspect ratio properties of carbon nanotubes to further enhance the sensitivity of humidity sensors.

Several studies have been done on the characteristics of CNTs. Rosca and Hoa [24] used scanning electron microscopy (SEM) to measure lengths, diameters, and aspect ratios of different MWCNTs, using the frequency distribution of each characteristic, and compared the results with the data given by the manufacturer. They also made bucky papers and studied the conductivity and percolation threshold of each MWCNT in their study. Guadagno et al. [12] synthesized 95% purified MWCNTs with catalytic carbon vapour deposition method. They used BET method and determined the specific surface area of the CNT to be 250-300 m^2/g. They also investigated the morphological parameters by HR-TEM, after dispersing the nanopowders by ultrasonic waves and doping them on a copper grid.

1.2.2.1 Synthesis

Different methods are utilized to synthesize single and multi-wall CNTs, including arc-discharge, laser ablation, gas catalytic growth from carbon monoxide, and chemical vapor deposition (CVD) from hydrocarbons. Arc-discharge technique, developed by Iijima, comprises of purely graphite rods as cathodes and anodes producing a stable arc. Carbon nanotube is synthesized and deposited on cathode along the fused material, and then it is purified by additional procedures. Laser ablation technique uses a laser beam to vaporize the graphite target held at 1200°C. The carbon nanotube

then deposits on a collector. The two mentioned techniques have very high costs and prohibit high-scale productions. In gas-phase and chemical vapour deposition techniques, the source of the carbon is the carbon carrying gas, which can be fed continually to the system by the flowing gas. CVD is currently the most commonly used method for the synthesis of CNTs, in which a hydrocarbon gas such as methane or carbon monoxide is decomposed on a metal substrate, and produces multiwall carbon nanotube. This technique offers high purity of CNT, and enables the production of aligned arrays of carbon nanotubes [14].

1.2.2.2   SWCNTs and MWCNTs

There are currently two types of CNTs on demand for different applications; single-walled carbon nanotubes (SWCNTs) and multi-walled carbon nanotubes (MWCNTs).

SWCNTs are conceptualized by rolling of a one-atom-thick layer of graphene around a hypothetical axis and into a seamless cylinder (Figure 1-5 a). MWCNTs consist of multiple layers of graphite rolled by two different configurations to form tubes. In the first configuration, known as Russian doll model, non-continuous graphite sheets are arranged in concentric cylinders and held by Van der Waals forces (Figure 1-5 b). The second arrangement, known as parchment model, includes an integral graphite sheet rolling around itself, resembling a scroll of newspaper. Double-wall CNTs (DWCNT) and cup-stacked CNTs (CSCNT) are also two other types of arrangements for CNTs with their unique properties and applications (Figure 1-5 c and d) [9,14].

Liang et al. [13] found SWCNTs to have a unique electronic structure, which alongside high curvature and surface area, leads to an improved wetting behavior when reinforcing epoxy composites. However, two advantages of MWCNTs over SWCNTs are that the multi-shell

structure is stiffer than the single-wall one, and there are more CVD processes available for large-scale synthesis of MWCNTs [12].
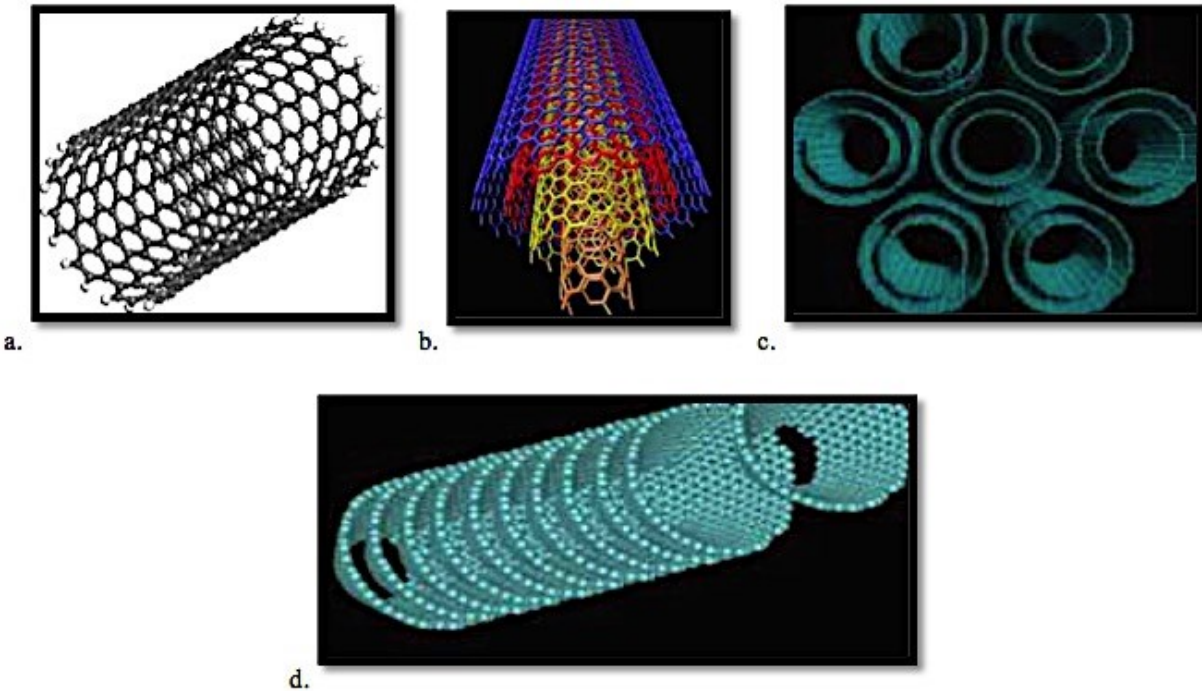
Figure 1-5 Computer-generated configurations of a) SWCNT, b) MWCNT, c) DWCNT, and d) CSCNT [9,13,25]

1.2.3 CNT Reinforced Epoxy Nanocomposites

The introduction of nanostructural reinforcements to the conventional fiber-reinforced epoxy composites to further enhance their superior properties has been the focus of many investigations. Carbon nanotubes are multifunctional materials that offer unique characteristics and versatility in design [23], and make way for the nanocomposites through many technologies ranging from microelectronics to aerospace [20]

The synergic effect of combining these two structural materials on the properties of the final composite is obtained through optimum contents of CNTs, and good dispersion of the particles allowing sufficient agglomeration of nanotubes.

1.2.3.1   Mixing and Dispersion

Carbon nanotubes, before being added to resin, resemble a black powder with particles very small in size and incredibly lightweight. They easily fly around in the air. On the other hand, when added to the epoxy resin, CNTs due to their tiny size and large surface area per unit volume, they have an intrinsic tendency to agglomerate. The tubes are held together by Van der Waals forces, and exhibit very low solubility in solvents. This entangled agglomeration disturbs the integrity of their excellent properties throughout the whole material [9]. It is also worth the mention that, adding small amounts of nanotubes to epoxy increases the viscosity of the mixture to a high extent, which may cause air voids being trapped in the material [9,26]. Therefore, advanced mixing techniques are required to obtain good dispersion of the nanotubes, followed by degassing procedures. Different techniques such as shear mixing, three-roll milling, dissolver disk, planetary mixer, and ultrasonic processing were utilized by researchers to add shear to the suspension and decompose the aggregated structures [24].

Rosca and Hoa [24] prepared homogenous nanocomposite mixtures using a three-roll milling device. They obtained highly conductive nanocomposites containing up to 8 wt.% CNT. Mactabi [14] and Naghashpour [19] used the same technique in their experiments. Starkova et al. [2] also employed a three-roll-milling device to mix the epoxy resin and the CNT, and then they added the hardener. Wichman et al. [26] used a mini-calender to disperse the nanoparticles in the epoxy, and they found that the degassing and the injection procedures required more time due to the increased viscosity. Barkoula and coworkers [23] deployed a torus mill device, consisting of a high-speed rotating disc and zirconium dioxide beads with diameters of 1.2 to 1.7 mm. The beads provide extra shear forces, and keep the vortex flow. They combined the mixing and degassing process by stirring the compound in a vacuum. Prolongo et al. [20] firstly dispersed CNTs in chloroform, and

then added the epoxy resin. They mixed the suspension with a simple mixer, followed by sonication of 50-60 Hz. The chloroform was removed by stirring at 90 °C, and finally, the curing agent was added. They induced a chemical reaction between the CNT and the epoxy by a thermal pre-curing treatment before adding the curing agent [20]. Cui et al. [27] initially mixed the epoxy and hardener components with a magnetic mixer, then introduced the conductive fillers and dispersed them by a solder cream mixer. They did not add any solvents to avoid air voids. Yu and coworkers [28] employed mechanical stirring followed by ultrasonication to disperse the CNT evenly in the curing agent. Then they added the epoxy resin and repeated the mechanical and ultrasonication mixing. The ultrasonication procedure was performed in an ice bath to prevent early curing due to high temperature. Finally, the mixture was degassed in a vacuum chamber. Guadagno et al. [12] conducted ultrasonication for the dispersion process of CNT and the resin, and then added the hardener. They used atomic force microscopy and observed that carbon nanotubes, depending on their concentration, were embedded and dispersed within the epoxy matrix singularly or in bundles.

1.2.3.2   Enhancement of Properties

Carbon nanotubes offer a high potential for upgrading properties of epoxies. Capability of enhancing mechanical and physical properties of the epoxies, as well as providing excellent electrical and thermal conductivity for them, has drawn the attention of many researchers to the incorporation of carbon nanotubes in these composites. In the following sections, findings of researchers regarding different properties of the epoxy composites will be summarized.

1.2.3.2.1 Physical

The addition of CNTs to the epoxy resin affects the curing process, the degree of the crosslinking, and the glass transition temperature. Guadagno et al. [12] observed the curing progress of epoxy nanocomposites using infrared spectroscopy, and showed that the presence of CNTs halves the disappearing time of epoxy bands and accelerates the curing. They also observed that the glass transition temperature increases with increasing MWCNTs, and they assumed this finding to be a result of good dispersion and interpenetration of CNTs in epoxy.

1.2.3.2.2 Mechanical

Carbon Nanotubes are pure C-C bonds and are very strong. They add strength and modulus to the composite, but at the same time reduce flexibility and increase rigidity. Small weight fractions of CNTs as low as 0.5 wt.% can improve damage tolerance properties of epoxies such as fracture toughness, impact strength, and fatigue life [23]. Barkoula et al. [23] believed that the enhancement of these properties is attributed to the addition of an interfacial area between the matrix and the nanotube, which dissipates the energy with different failure mechanisms at nanoscale, such as interfacial sliding, fiber pull-out, and bridging. Matthias and coworkers [17] compared the mechanical characteristics of epoxy adhesives reinforced with CNTs and Ag, and found that the storage modulus of the CNT increases with the CNT content, but at the end it is still remarkably lower than Ag-adhesives. Yu et al. [28] joined aluminum coupons with CNT reinforced epoxy adhesives, and tested the bonding strength and durability of the joints in 60°C water. They found that both properties, alongside the fracture toughness increased significantly with the addition of CNTs. However, with CNTs more than 1 wt.%, the initial fracture toughness decreased. Wichmann and coworkers [26] reinforced the epoxy in glass-fiber/epoxy composites with fumed silica and carbon black. They used the electrical conductivity property of these nanomaterials, and

applied an electrical field during the curing, which resulted in the orientation of nanofillers. By adding 0.3 wt.% CNT, they obtained 16% more shear strength. Guadagno et al. [12] obtained a higher elastic modulus for the MWCNT reinforced epoxy compared to the neat epoxy at elevated temperatures using dynamic-mechanical analysis. Liang et al. [13] used molecular dynamics (MD) simulation to explain the molecular interaction between (10,10) single-wall CNTs and EPON 862/EPIKURE W epoxy composites. They found that both resin and curing agent intercalate well with SWCNTs, aligning their aromatic ring planes and wrapping around the surface of the nanotube (Figure 1-6 a). They also theoretically demonstrated that epoxy crosslink networks fill into the cavity of the tubes, and lead to bridges that enhance the load transfer in nanocomposites (Figure 1-6 b)[13].
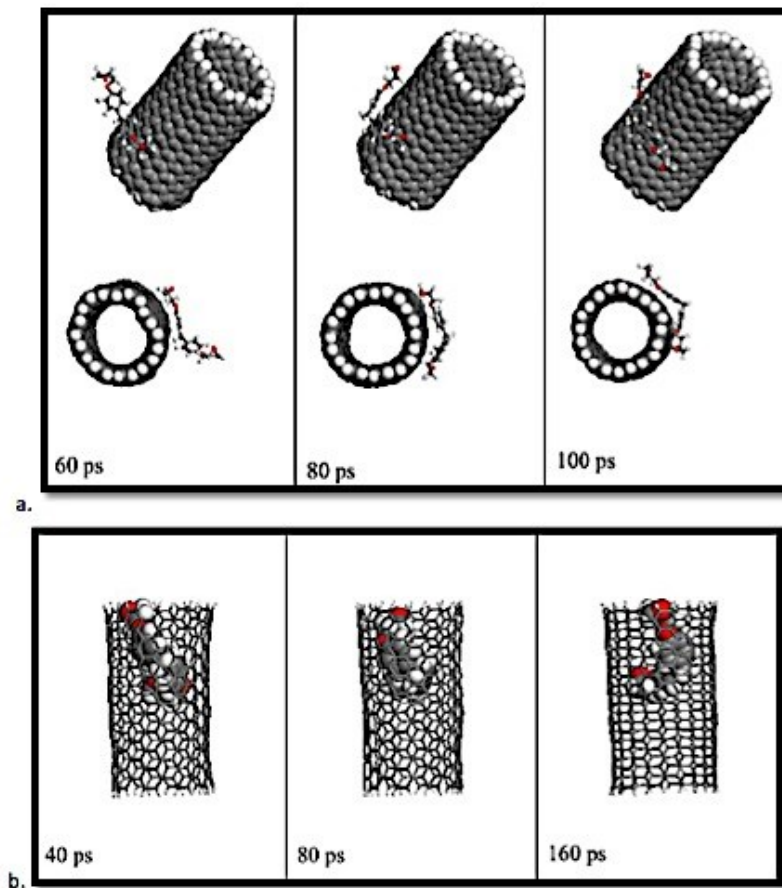
Figure 1-6 schematic of epoxy EPON 862 a) intercalating around SWCNT, b) filling into SWCNT [13]

1.2.3.2.3   Thermal

CNTs are thermally conductive. In manufacturing thick composite materials, carbon nanotubes are used as reinforcements to dissipate the heat throughout the thickness, and help the curing [1]. In terms of improving the thermal properties of epoxies, Yu et al. [28] demonstrated that the addition of 1 wt.% CNT to epoxy increases its thermal degradation temperature by 14 °C.

1.2.3.2.4   Electrical

One of the main motivations of researchers for reinforcing epoxy composites with CNTs is to obtain electrical conductivity [9]. Carbon nanotubes have unique electronic structures, are inherently conductive materials. They agglomerate and form conductive paths among each other with or without making connections. Their aspect ratio determines the extent of their agglomeration, their percolation behaviour, and electrical conductivity [13,24]. Yu et al. [28] found the percolation threshold of their CNT from a Chinese company to be to be 0.5 wt.%, while Rosca et al. [24] measured the percolation threshold of five different types of MWCNTs and obtained a range of 0.0117 to 0.1883 wt.%. Electrically conductive epoxy composites serve as candidates for electrically conductive adhesives (ECAs) in electronic packaging applications, and also for sensing and health monitoring purposes.

1.2.3.2.4.1 Electrically Conductive Adhesives

Requirements for lead-free, non-corrosive, light-weight ECAs in small electronic assemblies have drawn the attention of microelectronics industry to CNT reinforced epoxies [14,29]. They are high potential alternatives for metal-filled adhesives. They have also proven to have superior electro-mechanical properties and thermal conductivity [14,24,27]. Rosca et al. [30] induced electrical conductivity in epoxy adhesives for aluminum single lap joints by adding SWCNTs to obtain both electrical conductivity and improved bonding. They concluded that CNTs decrease the electrical

resistance of the lap joints by over ten orders of magnitude, but they also significantly decrease the fatigue life. For electronic packaging purposes, Cui et al. [27] produced tri-modal electrically conductive adhesives consisting of epoxy resin, micron silver flakes, micron silver spheres and acidified SWCNTs. They found that with the increase of ASWCNT, due to the formation of different conductive channels, the tri-modal ECAs' bulk resistivity firstly increased and then decreased.

1.2.3.2.4.2 *Structural Health Monitoring*

Incorporation of nanostructural fillers such as carbon nanotubes in epoxy composites increases the electrical conductivity and introduces the sensing functionality of the material, which has been taken advantage of as a health-monitoring technique [2]. Naghashpour [19] manufactured electrically conductive glass fiber/epoxy/MWCNT composites, and developed a structural health monitoring technique to detect damage in large polymer parts. He mounted grid points on the surface of the part, and measured the electrical resistance. Significant changes in the electrical resistance occurred at the grid points in the vicinity of damaged areas of the part. He also demonstrated that the uniformity of the electrical resistance is a result of the uniform distribution of MWCNTs, and the change in electrical resistance is more sensitive with smaller contents of CNTs above the percolation threshold [19]. Mactabi [14] developed an in-situ monitoring technique to observe the failure procedure, and predict the failure by the increase in electrical resistance of the lap joints in fatigue life testing. He showed that the change in resistance of lap joint remains lower than 10% of the initial value up to 80% of the fatigue life, and with the occurrence of crack propagation and interfacial delamination, the resistance exhibits a rapid increase.

1.2.3.2.4.3 Electrical Properties Measurement Techniques

For the study of electrical properties of CNT reinforced epoxy nanocomposites, such as electrical resistivity and electrical resistance, various methods have been employed by researchers. Among these methods, in-situ observation techniques have great popularity especially for structural health monitoring purposes. Probes are attached permanently to the test samples, in a way that the contact resistance is minimized, to pass the current and record the voltage. Rosca et al. [30], Mactabi [14], used 2-probe and 4-probe configurations directly attached to two aluminum substrates joined by CNT reinforced epoxy adhesive. Since the conductivity of the aluminum is considerably higher that the adhesive, the resistance measured by the probes referred to that of the adhesive and its interface with the aluminum coupons [14]. Aiming for the immersion of samples in water, Barkoula et al. [23] grinded the two ends of their epoxy nanocomposite coupons, and coated them with conductive silver paint. Then they pasted electrodes to the ends with conductive epoxy glue and covered them with silicone in an effort to eliminate the deterioration of the electrodes in water. They passed the electrodes through sealed holes in the lid of the container, and did not remove them throughout the course of experiment.

Van der Pauw method is an electrical resistivity and Hall coefficient measuring system. Naghashpour [19] used the method of Van der Pauw in his research to measure the volume electrical resistivity of MWCNT reinforced glass-fiber/epoxy composite plates.

1.2.4 Moisture Absorption of Neat and CNT Reinforced Epoxy Composites

Epoxy is a common resin matrix used in structural composites with a wide range of applications in aerospace, automobile, and civil industries. It is also used as adhesive joint with different purposes. In most of its applications however, there is a strong possibility for the material to be

exposed to extreme environmental conditions, including high relative humidity and elevated temperatures, where the durability of the material becomes a big concern [31,32]. Polymers depending on their functional groups can be hydrophilic or hydrophobic. Epoxies due to the existence of oxygen atoms on their surface have hydrogen-bonding characteristics, and are highly polar [33]. When cured, they have a tendency to absorb water, gain weight, and swell, which results in altering their properties. Therefore, the water absorption behaviour of epoxies is one of the reliability concerns of these materials, and is a topic of great importance for researchers [2,33,34].

1.2.4.1 Mechanism of water transport

Several researches have been conducted on the subject of water transport in Epoxy systems. There are two main concepts explaining the entering and movement of water molecules inside the epoxy structure; water uptake and diffusivity. In the following sections, an explanation of each is provided, followed by the findings of various researchers.

1.2.4.1.1 Water Uptake

When the substrate of a solid material is exposed to humidity or immersed into water, molecules of water diffuse through the surface and inside the material. Water uptake (W_t) is defined by the weight gain of samples due to this transport, and is measured by dividing the difference between the current weight (m_t) and the initial weight (m_0) by the initial weight of the tested sample (Eq. 1.1).

$$W_t\,(\%) = \frac{m_t - m_0}{m_0}\,x100 \tag{1.1}$$

17

1.2.4.1.2 Diffusivity

The term "diffusion" refers to the physical process of random movement of molecules, flowing from a high-concentration region to a low-concentration one. The rate of water penetrating deep into the epoxy composite is shown by diffusivity, and it depends on two parameters:

1. The mobility or dynamics of the polymer chains, which mainly depends on temperature
2. The tortuosity of the available paths for diffusion, which is dominated by the presence of particles.

The water uptake is plotted against the square root of time of water immersion or humidity exposing, exhibiting an upward trend that resembles the curve of Fick's first law of diffusion. Depending on the temperature, the water uptake curve of epoxies can coincide very closely with Fick's law [2,4,35,36]. Fickian model is a common approach for explaining water absorption because of its simplicity. It only considers the parameter of diffusion and neglects the parameters of degradation and molecular relaxation [2]. The Fickian upward trend includes a linear increase at first, followed by a non-linear rise, as it gets closer to saturation. The rate of weight gain falls gradually into a nonlinear flow until saturation is reached. Non-Fickian behaviours often happen when the relaxation of the polymer affects the water uptake [33]. Several non-Fickian models have also been approached to explain the water absorption behaviour of materials in glassy state, including Langmuir, Jacob's-Jones, Relaxation, and Time-variable models. Langmuir model, also known as Carter and Kibler model, considers the effect of both free water and bound water phases in the absorption procedure [2,36,37], whereas Jacob's-Jones model assumes that there are two separate phases with different densities and different sorption behaviours in the material [36]. Relaxation model employs the viscoelasticity characteristics of the polymer to explain the

procedure [2,4], while the Time-variable model considers a diffusivity that decreases with time in proportion to its current value [36].

For the cases that the width and length of sample plates are significantly larger than their thickness, diffusion is considered as a one-dimensional process, and is explained by the following equations [2,5,31,36,38,40] (Eq. 1.2 and 1.3):

$$D = \frac{\pi}{16} \left(\frac{a}{W_\infty/W_0}\right)^2 K^2 \tag{1.2}$$

$$D = D_0 \exp\left(-\frac{Q}{R_g T}\right) \tag{1.3}$$

Where D is the diffusion coefficient, W_∞ and W_0 are weight gains at saturation and dry conditions, respectively, a is the thickness of the plate, and K is the slope of the linear region of the plot of W_t versus the square root of time. In Eq. 1.3, D_0 is a constant equal to D at 1/T=0, Q is the activation energy of diffusion, R_g is the universal gas constant, and T is the absolute temperature of diffusion [2].

As mentioned before, moisture rarely has a favourable influence on the properties of composite materials. Water molecules diffuse into the material, act as plasticizers, and increase the mobility of the polymer chains. They cause changes in the molecular structure, which could be seen as an increase in the space between the polymer molecules and swelling [11]. Water molecules are also capable of forming hydrogen bonds with polymers and other components in the material, and alter the structure. In an approach to explaining the mechanism of water transport in epoxies, it was considered that two types of water exist. The first type of water is assumed to enter the material and occupy the free space between epoxy molecules, without any formation of bonds, whereas the second type emphasizes on specific interactions between the polymer and the penetrant molecule,

i.e. strong hydrogen bonds between water and hydrophilic functional groups such as hydroxyl and amine [2,39,40]. The water saturation level of the polymer depends on the available free volume and the open hydrogen bonds, while the diffusivity depends mainly on the free volume of the polymer [2]. Zhou et al. [40] used solid-state nuclear magnetic resonance (NMR) to detect the status of water molecules in contact with epoxy molecules. Taking into account the NMR results, Zhou and coworkers demonstrated that there are two main types of water found inside the samples. At the initial stages of the exposure of epoxy to water, there exist free water molecules with no bonds formed with epoxy. They move independently among epoxy molecules and fill up free spaces. But the polar groups of water and epoxy in the material eventually begin to attract each other. Free water transforms into bound water, breaks the Van der Waals forces and forms hydrogen bonds with the hydrophilic functional groups such as hydroxyls and amines. These water molecules, also known as bound water type I, act as plasticisers and lead to the movement of the polymer chains. They form only one hydrogen bond with the -OH functional groups in epoxy or – NH in amine (Figure 1-7 a).
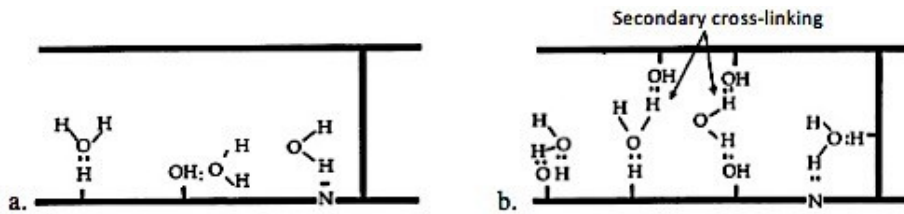
Figure 1-7 Possible configuration of bound water types in epoxy a) bound water type I, b) bound water type II [40]

In the procedure of desorption, the bond is removed at a moderate temperature as the temperature provided for absorption, and the water escapes the material. There is also another type of bound water known as type II, which forms more than one hydrogen bond with the epoxy and the amine, and acts as a bridge between structural segments (Figure 1-7 b). Bound water type II does not have

a significant effect on the volume change of the material [2,40]. It requires more effort to be removed from the material; its relative activation energy is more than that of type I bound water.

For the desorption procedure, Zhou et al. [40] performed a two-step experiment; first, they allowed the samples to dry at a temperature below T_g, i.e. the same temperature as the absorption, and then they increased the temperature to above T_g for all the remaining water to be removed from the material. The first step provided enough time for the bound water type I to escape the material, and once the samples stopped losing weight, the temperature was increased to a value above T_g, which supplied the activation energy to break multiple hydrogen bonds (Figure 1-8). The NMR results in the study of Zhou and coworkers also showed that free water does not stay inside the sample as free water for long, it eventually becomes bound water type I [40].
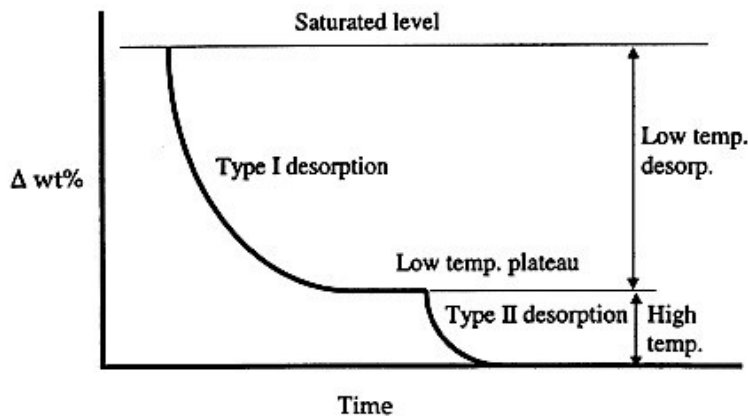
Figure 1-8 Schematic of water desorption process [40]

1.2.4.2   Effect of Water Absorption on Properties of Neat Epoxy Composites

The gradual structural changes caused by plasticisation and secondary cross-linkings influence the properties and the performance of the composites. These long-term changes have been the subject of study of many researchers, and can be categorized into changes in dimensional, physical, and mechanical properties of the epoxy composites.

Formation of hydrogen bonds between water molecules and hydroxyl groups, and plasticising the polymer chains alters the structure of the epoxy [37]. Starkova and coworkers [2] showed that this plasticization results in the change of dimensions and swelling of the material, as well as diminishing the glass transition temperature, while Zhou et al. [41] examined the behaviour of three types of epoxies after saturation and discovered that there is a considerable drop in the T_g with the absorption of water, due to the plasticizing effect of type I bound water. But once the saturation is reached, the T_g gradually increases again. This was considered as the contribution of type II bound water to secondary cross-linking (Figure 1-9) [41].
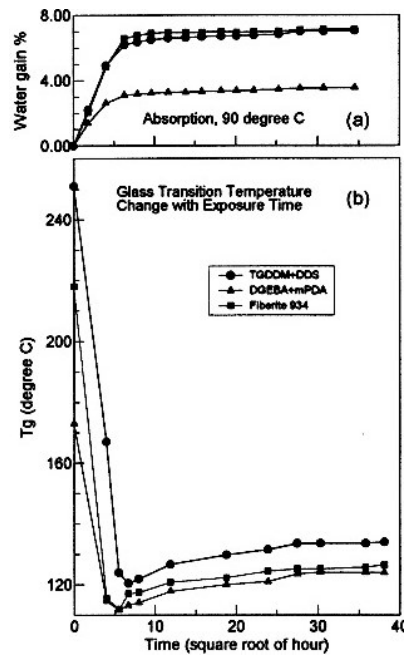
Figure 1-9 Changes in glass transition temperature at pre- and post-saturation stages of immersion [41]

Regarding mechanical properties, Kwei [42] concluded by comparing the strength of epoxy resins under dry and humid conditions that, water disrupts the interchain hydrogen bonding and causes the deterioration of mechanical properties [3,42]. Also, according to the theory of fracture of Beuche [43], the disruption of interchain hydrogen bonding causes "the jump frequency of the

22

polymer segments" to increase. This phenomenon decreases the tensile strength and the fatigue life of epoxies [3,42,43]. Lin et al. [4] conducted a series of sorption, desorption, and resorption experiments on epoxy composites, and demonstrated that after the first cycle of sorption and desorption, the tensile elastic modulus and strength were not entirely recoverable (Figure 1-10 a). They also found that the resorption process is faster than desorption, and the desorption is faster than the sorption [4], and also the level of saturation in the resorption procedure is higher than the first sorption cycle. They considered both these effects to be a result of increasing the free volume by the penetration of moisture (Figure 1-10 b) [4].
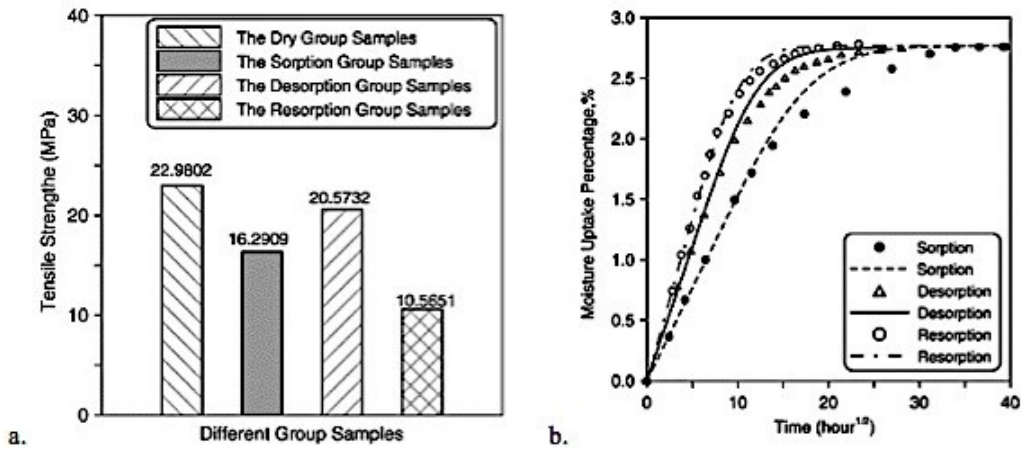
Figure 1-10 a) Tensile strength and b) Moisture uptake of epoxy composite at sorption, desorption, and resorption hygrothermal cycles [4]

In another study, Dutta [21] obtained a desorption rate five times faster than the absorption rate of their epoxy samples. He also observed that the T_g of the epoxy decreased by 20 °C in the absorption procedure, and only gained 10 °C back after being fully desorbed. Mubashar et al [32] used epoxy adhesive for single lap joints, and found that the tensile strength of the adhesive and the failure strength of the joints degraded with the absorption of water, but when dried, most of the joint strength was recovered.

Xiao et al. [44] investigated the effect of water absorption on the swelling behaviour of the epoxy composites, and found that, initially, the rate of swelling is less than that of water uptake, but it equalizes later. They also showed that by desorbing water out of epoxy, the swelling is not completely recoverable, and some residual volume increase is evident in the epoxy, which is a result of the alteration of the molecular structure as well as the possibility of some water still existing in the material [44]. In another study, Ardebili et al [6] plotted hygroscopic strain of four types of epoxies against the water uptake, which proved to be a linear trend except from the initial stages of the desorption procedures.

1.2.4.3   The Contribution of CNTs to Water Absorption in Epoxy Nanocomposites

Even a very small inclusion of CNTs in the composites affects its water absorption behaviour. The barrier effect of CNTs will decrease the rate of water uptake, and will improve the overall mechanical properties of the moist nanocomposite [2].

There is no exact mechanism proved to be explaining the transport of water molecules in between the CNT molecules inside the Epoxy. Starkova et al. [2] investigated the water absorption behaviour of a DGEBA-based epoxy system reinforced by Bayer MWCNT in a wide range of relative humidity and temperatures. They made several conclusions worth pointing out, which will be categorized as followed: 1) The level of water uptake of the samples regardless of the amount of CNT remained unchanged, which was assumed to be the counterbalancing of higher number of polar bonds available for water molecules, and lower mobility of polymers. 2) The saturation level of the plates increased with the increase in temperature. They considered it to be a result of increase in segment mobility of the polymer molecules in higher temperatures. 3) The addition of up to 1 wt.% MWCNT decreased the diffusivity of the material two times compared to that of neat epoxy,

due to the increased tortuosity of the diffusion path and the barrier effect of the CNT, and also the assumption that restricting movements of polymer chain by CNTs will delay their relaxation. However, this positive effect diminishes with increasing the temperature and the mobility of polymer chains and water molecules. To better demonstrate this effect, they plotted the natural logarithm of diffusion coefficient against 1/T and calculated the activation energy of diffusion of samples with 0.5 wt.% CNT to be 16% more than that of neat epoxy, which shows that CNTs hinder the diffusion of water inside the composite and more energy is needed for this process. But when the temperature increases, water molecules become more active and the diffusion takes place more easily. 4) Swelling happens with water uptake, regardless of the CNT content. The swelling coefficient $\beta=\Delta\varepsilon_{sw}/\Delta W$ (%/%) was found to be 0.24. 5) The glass transition temperature of the nanocomposite compared to the neat polymer remains unchanged, and in both cases a 20 °C reduction in the T_g was observed at saturation. Because the effects of lower degree of cure, caused by the presence of CNTs, and the restriction of the mobility of polymer chains neutralize each other. 6) The existence of CNT in the composite while exposing to humid conditions helps the glassy modulus to decrease less severely, since less plasticisation occurs in the case of the nanocomposites due to the higher contribution of type II bound water. To investigate this matter, Starkova and coworkers performed tensile mode dynamic mechanical and thermal analysis (DMTA) on dry and saturated plates [2]. Figure 1-11 simulates the difference between the free volume in neat epoxy and the nanocomposite [2].
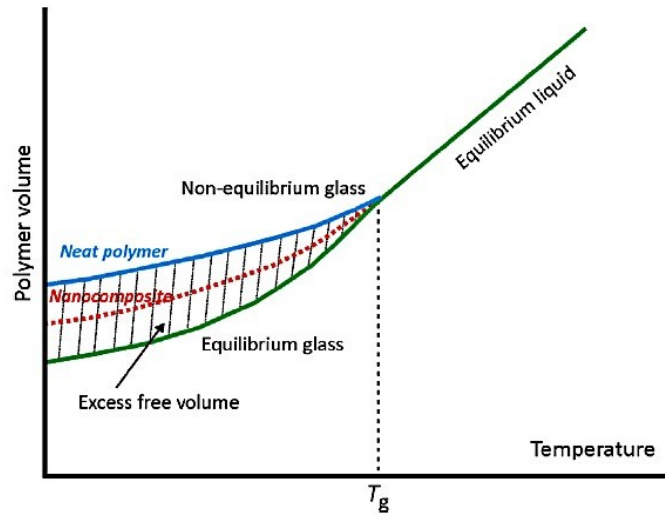
Figure 1-11 Volume vs. temperature of neat polymer and CNT reinforced nanocomposite [2]

According to this figure, the excess free volume in the polymer is the difference between the volume that is merely occupied by polymer molecules, and the actual volume of the sample at a given temperature, which also depends of the degree of cure and the physical aging of the composite. With the addition of CNTs to the plates, the excess free volume decreases, since the movement of polymer chains is limited. The extent of reduction also depends on the volume fraction and the agglomeration of carbon nanotubes.

Prolongo et al. [20] showed that the moisture saturation level of epoxy considerably decreases with the addition of CNTs due to the high hydrophobicity and strong barrier properties of CNTs. They also maintained that the mechanical strength of the composite deteriorates as a result of plasticisation, but after saturation, the composite gains its strength to some extent with the help of secondary cross-linkings.

1.2.4.4 Influence of Water Absorption on the Electrical Properties of CNT-Reinforced
        Nanocomposites

Electrically conductive epoxy nanocomposites are fabricated with the addition of carbon nanotubes to epoxy. They are aimed for electronic packaging applications as well as structural health monitoring methods. The electrical properties of these nanocomposites are susceptible to hostile environments, and when exposed, are altered in adverse ways. Ling et al. [22] applied a thin layer of SWCNT film on a pair of gold (Au) electrodes and investigated the humidity-dependent conductance of its network. They found that SWCNTs separate linearly with the humidity levels, resulting in a reduction in their electrical conductance.

As mentioned before, Barkoula et al. [23] related the improvement in the mechanical properties of CNT reinforced epoxy composites to the addition of an interfacial area between the CNTs and the matrix. However, they also noted that this additional interface increases the ability of the matrix to absorb more moisture, and causes the environmental durability of the material to be altered. They made CNT reinforced epoxy plates with 0.3, 0.5, and 1 wt.% contents of CNT, immersed them in water, and measured their in-situ electrical resistance at different time intervals through the length of the material. For all CNT concentrations, they observed that, the electrical resistance initially increased and reached a peak, and then monotonically decreased until the end of immersion (Figure 1-12). In all samples, the value of the electrical resistance at saturation was even less than that of zero water uptake. It is evident from the figure that the drops were more pronounced for samples with less CNT concentrations [23]. They did not provide any information on the dimensions of the samples, and no explanation of the mechanism of electrical resistivity decrease was offered.
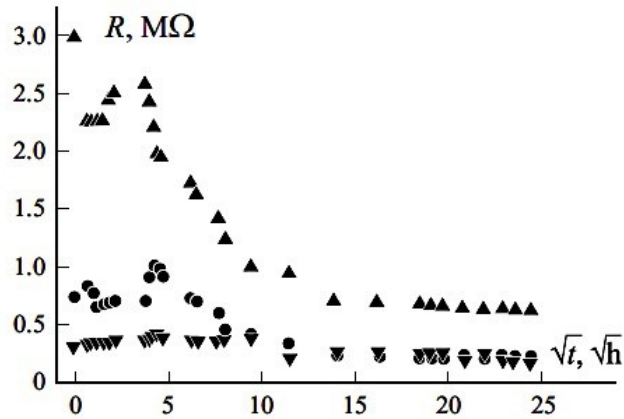
Figure 1-12 Electrical resistance behaviour of CNT reinforced epoxy nanocomposites immersed in 80 °C distilled water for 0.3 (▲), 0.5 (●), and 1(▼) wt.% CNT concentrations [23].

1.3 Problem Definition and Objective

Epoxy resins are considered as one of the most common matrices for structural composites because of their superior mechanical, physical, chemical, and thermal characteristics. To further improve those properties, and specifically to induce electrically conductive in epoxies, carbon nanotubes are added to the system. The properties, advantages, and applications of epoxies have been the subjects of study by a many researchers, examples of which were presented in this literature review. Epoxies are receptive to humid environments, and their structure and properties can be altered with the diffusion of water molecules. Various researchers have contributed their studies to the analysis of the mechanism of water transport, as well as the changes occurred in the mechanical, physical, and thermal characteristics of both neat and CNT reinforced epoxy composites. Efforts have been made to clarify the role of carbon nanotubes in reducing or strengthening the destructive effect of water absorption in epoxies. However, a lack of research is evident in the area of electrical properties and moisture. When conductive epoxy nanocomposites are exposed to humidity, the alteration of their structure affects their electrical conductivity behaviour. Only one research by Barkoula et al [23] was found devoted to finding a relationship

28

between the structural changes in the conductive epoxy nanocomposite and its electrical properties in a humid environment, but the authors did not provide dimensions for the sample, nor they provided any explanation for the reason why the electrical resistance decreased with water absorption.

The objectives of this thesis are as follows:

- To study the mechanism of water transport into MWCNT reinforced epoxy nanocomposites, and its role in altering the electrical resistivity behaviour of the material.
- To find relationships between the changes in water uptake and diffusivity, thickness, and electrical resistivity.
- To propose a theory to explain the electrical resistivity behaviour of the material with water absorption.
- To investigate the recovery of the properties through desorption experiments.

1.4 Thesis Contents

Chapter One provides a general overview of epoxy composites, carbon nanotubes, and carbon nanotube reinforced epoxy nanocomposites, followed by their superior properties and limitations. A detailed literature review is provided on the studies related to moisture absorption and electrical resistivity behavior of CNT reinforced epoxy nanocomposites conducted by other researchers. The motivations and objectives of this thesis project are given at the end of this chapter, and thesis contents are mentioned.

Experimental aspects of the project are explained in Chapter Two. Details about the preparation steps of sample plates, the quality control observation of the prepared samples, and all the measurement techniques for the purpose of the research are given in this chapter.

Chapter Three demonstrates the water uptake, thickness change, and electrical resistivity results of both water and oil absorption experiments gathered in graphs and tables. Comparisons of the results of different immersion temperatures and nanotube types are also provided in this chapter. A schematic electrical resistance circuit model is proposed to explain the role of water, air, and MWCNT conductive paths in passing the current. Desorption results of saturated MWCNT reinforced epoxy nanocomposites are also demonstrated, and the recovery of their weight gain and electrical resistivity is studied.

In Chapter Four, a comprehensive conclusion of the thesis project, its contributions, and suggested future works are presented.

2 Experimental

2.1 Introduction

For the purpose of this research, MWCNT reinforced epoxy nanocomposite plates with defined dimensions were fabricated, and measurements and tests were conducted. A detailed explanation of fabrication and measurement procedures are provided in the following sections.

2.2 Materials

The three main contents of each sample plate were epoxy resin, curing agent, and Carbon Nanotubes. The details are provided below.
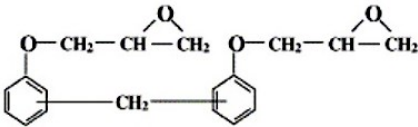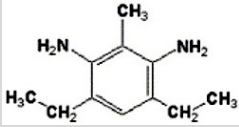
2.2.1 Epoxy Resin and Curing Agent

The Epoxy resin used in this research was EPON™ Resin 862 or Diglycidyl Ether of Bisphenol F supplied by Momentive, USA. EPON 862 is a transparent liquid resin, manufactured from the reaction of epichlorohydrin and bisphenol F. It does not contain any diluents or modifiers, offers a good balance of mechanical and electrical properties, and is a well-qualified material for chemical resistant tank linings, fiber reinforced pipes, molding compounds, electrical adhesives, etc. [47]. The curing agent was chosen to be EPIKURE™ W or Diethyltoluenediamine (DETDA), an aromatic amine hardener with low viscosity. The molecular structure and physical properties of EPON 862 and EPIKURE W are presented in Table 2-1 [14,47].

The selection of this epoxy system was made according to the several advantages of the resin. EPON 862 is intrinsically a low viscosity resin. Since the addition of carbon nanotube considerably

increases the viscosity of the uncured mixture, the viscosity of the epoxy system should be sufficiently low to facilitate and accelerate the injection molding procedure. Moreover, EPON 862 is a high temperature curing resin offering excellent mechanical and adhesive properties and chemical resistance, and is a commonly used resin in industry as well as among researchers.

Table 2-1 Molecular structure and physical properties of EPON 862 resin and Epikure W curing agent [10]

Component	EPON™ 862	EPIKURE™ W
Molecule	Diglycidyl Ether of Bisphenol F (DGEBF)	Diethyltoluenediamine (DETDA)
Molecular Structure		
Density (g/cm³)	1.17	1.02
Viscosity at 25 °C (cp)	25-45	5-20
Equivalent weight (g/eq)	165-173	200
Flash Point (°C)	150	135

2.2.2 Silicone Rubber and Engine Oil

Silicone rubber was chosen as an alternative for the matrix to intensify swelling and study its influence on the electrical resistivity of the nanocomposite.

2.2.2.1 Background

Sylgard 184 Silicone elastomer base and curing agent were used as the matrix of nanocomposite in this experiment. Sylgard 184 is a polydimethylsiloxane elastomer (PDMS) with Si-O bonds in its main chains, which is traditionally considered as a hydrophobic material. It is frequently used for its moisture barrier properties, high chemical and mechanical stability, and high thermal resistance over a wide range of temperatures [48,49]. This silicone rubber offers good dielectric

properties, and is qualified for applications such as power supplies, connectors and sensors, amplifiers, and LED lighting encapsulations [50]. Abd-El Salam et al. [49] reinforced this elastomer with electrically conductive fillers including carbon black and graphite, and fabricated electrically conductive silicone rubber components. They investigated the conductivity behavior of this material with swelling, and found that by increasing the volume of silicone rubber, the electrical conductivity decreases.

2.2.2.2   Selection of Immersion Liquid

As shown in the literature and in all the previous experiments, epoxy can absorb up to 2 wt.% water. On the other hand, silicone rubber, due to its hydrophobic properties, showed a significant resistance against absorbing water, and after 24 hours of immersion, no weight gain was observed. Table 2-2 provides a summary of all the assessments for choosing a liquid that can be absorbed by silicone rubber. The procedure of immersion in acetone, as an alternative to water, proved to be unsuccessful, since acetone dissolves and degrades silicone rubber. Iso-propyl alcohol was absorbed by both epoxy and silicone rubber.

Table 2-2 Assessment of the absorption behavior of epoxy and silicone rubber in different solvents.

Solvent	Epoxy	Silicone Rubber	Conclusion
Water	Slow absorption of up to 2%	No absorption after 24 hours	Only effective on epoxy
Acetone	Fast absorption, fast evaporation	Degraded matrix	Only effective on epoxy
Iso-Propyl Alcohol	Fast absorption, fast evaporation	Fast absorption, fast evaporation	No enough time for measurements
Engine Oil	No absorption after 24 hours	Fast absorption of up to 9% in 24 hours	Only effective on Silicone Rubber

However, the extremely high volatility of the alcohol made it impossible to measure the desired properties in such short time. Finally, MotoMaster 2-Cycle Engine Oil was used as an alternative to water, and although no weight gain was observed in the epoxy nanocomposite, silicone rubber gained the considerable amount of 9% of its initial weight after only 24 hours of immersion.

It is noteworthy that, neither epoxy dissolves in water, nor silicone rubber in engine oil. And the only possible cause of swelling is the occurrence of plasticization inside the batch of material. Bearing in mind this assumption and according to all-the-above findings, it was decided to make carbon nanotube reinforced silicone rubber nanocomposites, immerse them in engine oil, and conduct experiments comparable to those of epoxies in water.

2.2.3 Carbon Nanotubes

Multi-walled carbon nanotubes were provided from two different suppliers. The first two experiments were conducted using Baytubes® C150P MWCNT purchased from Bayer, Germany. The fabricated samples exhibited very high resistivity values, and noticeable standard deviations were obtained for five samples with the same CNT content. Therefore, to acquire higher conductivity and precision in the electrical resistivity of the samples and to narrow the variability of the values, this CNT was later replaced by Industrial Grade MWCNT supplied by NanoLab Inc., USA. The physical and electrical characteristics are both carbon nanotubes are summarized in Table 2-3. As can be seen from the table, the aspect ratio of the NLIG carbon nanotube is more than five times bigger than that of C150P, which results in an improved agglomeration of nanotubes, more convenient formation of conductive paths, and finally, lower percolation threshold [24].

Table 2-3 Comparison of dimensional and percolation properties of Baytubes® C150P and NanoLab Industrial Grade (NLIG) MWCNTs [24].

	Length (μm)	Diameter (nm)	Aspect Ratio	Percolation Threshold p_c (wt.%)	Intrinsic Conductivity σ_0 (S/m)
C150P	0.61	11.61	52.7	0.1883	3981.2
NLIG	3.34	11.54	289.4	0.0117	23075.3

Three concentrations of MWCNT, as mentioned in Table 2-4, were considered for the epoxy system. Since the percolation threshold of the C150P was nearly 0.2 wt.%, the minimum CNT content was chosen to be 0.3 wt.%, in order to obtain stable electrical conductivity. Other samples were made with 0.5 and 1 wt.% CNT, alongside samples with merely neat epoxy.

Table 2-4 Epoxy/CNT systems used for the fabrication of samples- five plates of each concentration were fabricated.

CNT Concentrations (wt.%)
0 wt.% (Neat Epoxy)
0.3 wt.%
0.5 wt.%
1 wt.%

2.3 Sample Fabrication Procedure

The fabrication procedure consists of mixing and dispersing of the three components, injection molding, curing, and final trimming.

2.3.1   Mixing and Dispersion

As mentioned in Chapter One, carbon nanotubes are extremely lightweight black particles small in size, but large in surface area per unit volume. When added to the epoxy resin, they have a strong tendency to agglomerate and stay entangled. Therefore, untangling and dispersing these agglomerations in order to obtain integrity of the properties throughout the entire material is rather challenging, and requires an advanced technique. Moreover, carbon nanotubes increase the viscosity of the mixture and hinder the easy elimination of air bubbles formed inside the material. Thus, additional vacuum assisted degassing procedures are required to avoid any trapped air voids in the final products.

The first step in the preparation of the material was to mix the MWCNT with the resin. The ratio of the curing agent to the resin as advised by the manufacturer was 26.4%. For each MWCNT concentration 5 plates were made. The prepared mixture was injected into five closed molds each with the capacity of 8 g. The total weight of each mixture was chosen to be 60 g, higher than the expected weight, since material loss was inevitable during different preparation procedures. The amount of each component was obtained using the calculations below (Eq. 2.1 – 2.4).

$$M_r + M_{ca} + M_{CNT} = M_T \tag{2.1}$$

$$M_{ca} = 0.264\ M_r \tag{2.2}$$

$$M_{CNT} = a.\ M_T \tag{2.3}$$

$$1.264\ M_r = (1\text{-}a)\ M_T \tag{2.4}$$

where M_r, M_{ca}, and M_{CNT} are the masses of resin, curing agent, and MWCNT, respectively, M_T is the total weight of the mixture, and a represents the concentration of MWCNT.

The calculated amount of epoxy resin and MWCNT were added together in a beaker. To avoid partial curing of the epoxy, the curing agent was kept aside and added to the mixture in the subsequent stages of preparation. The combination of resin and MWCNT were mixed manually by rotation until no obvious cluster of MWCNTs were evident. The mixture then underwent the procedure of three-roll milling using the laboratory scale three-roll mill EXAKT 80E, from EXAKT Technologies Inc., Germany (Figure 2-1 a).
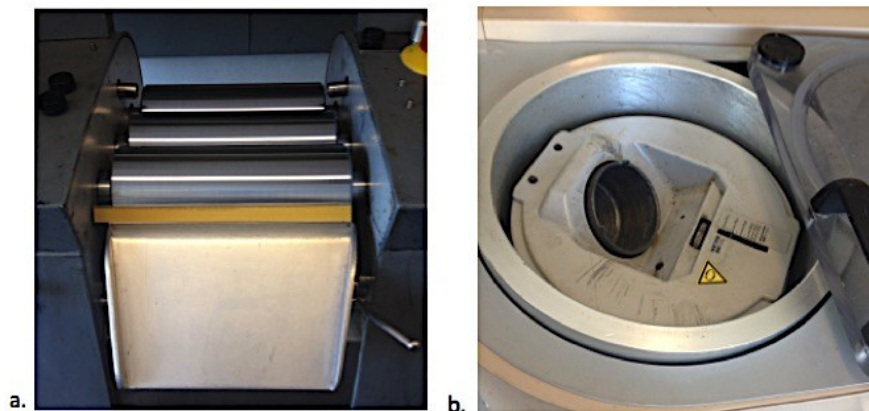
Figure 2-1 a) Three-roll mill, and b) vacuum mixer devices

As mentioned in the literature, Rosca and Hoa [24] investigated three dominating parameters of speed of rotation, the gap space between the mills, and the number of passes for the three-roll milling device and came up with an optimum combination of three to obtain excellent dispersion, and high electrical conductivity. Figure 2-2 includes a caption of the different combinations of the three parameters, providing different shear mixing intensities, and the electrical conductivity results they obtained for different CNT types [24].

Figure 2-2 a) Four mixing sequences b) electrical conductivities obtained by the mixing sequences for four types of CNTs, by three-roll-milling device [24].

The optimum combination of three parameters that provides the best dispersion of carbon nanotubes in the epoxy resin, as shown in Table 2-5, was employed for the purpose of this thesis, too. Careful calculations were carried out again, and the right amount of curing agent was then added to the mixture. After blending it manually, the mixture was placed in a THINKY Conditioning Vacuum Mixer ARV-200 (Figure 2-1 b), and was vacuum mixed for 90 seconds with the rotation speed of 1900 rpm. This device provided a vacuum of 5 mmHg alongside a centrifugal force that not only homogenized the material, but also extracted the air bubbles trapped inside the blend. The vacuum mixing also increased the temperature of the mixture, due to shear forces, which resulted in decreased viscosity and easier injection in the molds.

Table 2-5 Optimum combination of three parameters for the three-roll milling procedure, provided by Rosca and Hoa [24].

[Gap space (μm), Number of passes, Rotation speed (rpm)]
[50, 2, 100]
[20, 1, 100]
[10, 3, 100]

2.3.2 Molds Preparation

Stainless steel molds with smooth surfaces were prepared as shown in Figure 2-3 a, and equipped with rubbers on the edges to provide complete sealing. They were coated with LOCTITE Frekote 770-NC releasing agent to avoid sticking of the material to the surface. The four corners were fastened with screws using a torque gauge screwdriver to have uniform forces on the corners. Figure 2-3 b shows the configuration of the closed molds. As can be seen from Figure 2-4, a cut on the upper side of the rubber was punctured to provide a path for the injection of the material.
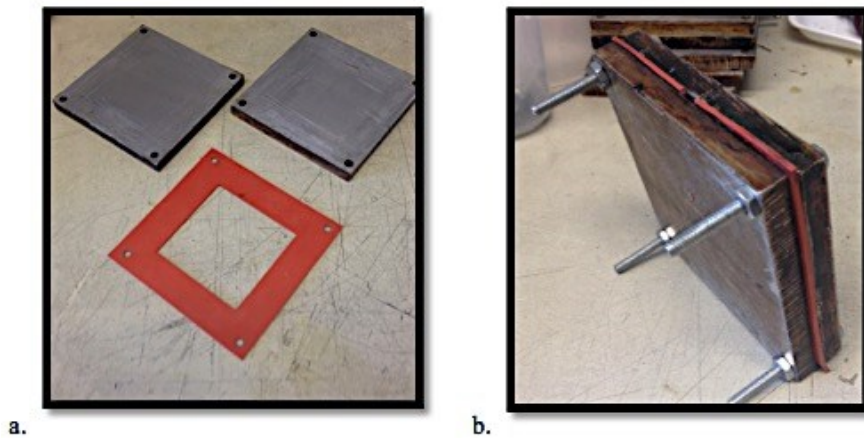
Figure 2-3 a) Stainless steel molds and sealing rubber, and b) the configuration of the closed mold.
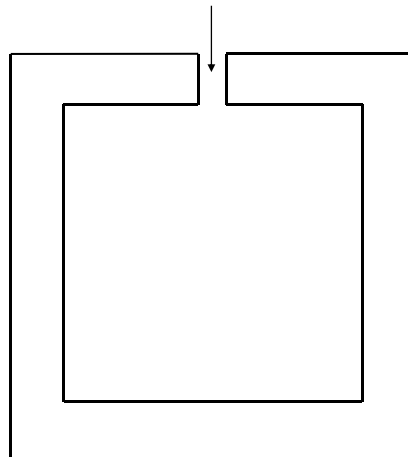
Figure 2-4 Configuration of the mold puncture for injection

For each batch of material with a specified MWCNT concentration, five molds were employed. The mixture was injected into the molds through a syringe very gradually, letting the air come out of the mold. The molds were prepared and placed in the oven.

2.3.3   Curing and Trimming

The mold assemblies were held vertically in the oven with the injection cut on top, to facilitate the air escape, if any, during the curing procedure. The curing cycle was 2 hours at 177 °C, as advised by the manufacturer. After cooling down, the panels were separated from the molds. For each of the MWCNT contents, i.e. 0, 0.3, 0.5, and 1 wt.%, five panels with thicknesses of approximately 1.5 mm were obtained. The thickness of the panels was deliberately made small to omit the edge effects, and to be able to use a two-dimensional method for measuring the electrical resistivity. Panels were cut, using an electrical rotating saw, into square plates of 45x45 mm. Figure 2-5 shows the final cut and trimmed plate, ready to be dried, and then immersed in the water bath.
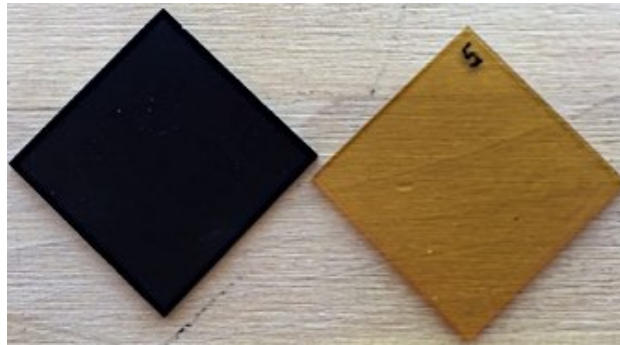
Figure 2-5 CNT reinforced (left) and neat (right) prepared plates for water immersion procedure.

For the fabrication of silicone rubber plates, mixtures of silicone rubber and curing agent containing 0.3, 0.5, and 1 wt.% IG MWCNT, along with a mixture of neat silicone rubber, produced by the same procedure as for epoxy plates, were injected into the moulds. The curing

took place in an oven at 100 °C for one hour. Plates were then cut and trimmed to the same dimensions as for the epoxy plates.

2.4 Immersion and Desorption Procedures

The fabricated plates were first dried, and then immersed in water, and their different properties were measured periodically. The immersion procedures are explained in the following sections. For the desorption experiments, plates were taken out of water and again, their properties were measured regularly.

2.4.1 Initial Drying of the Plates

In order to get the initial weight and electrical resistance data, the prepared epoxy and SR plates needed to obtain full dryness. For this matter, they were placed in an oven at 110 °C for more than 24 hours, and they were weighed every four hours until a constant minimum weight was obtained. They were then kept in a desiccator cabinet before immersing into water, and their dry-condition weight, thickness, and electrical resistivity were measured and recorded.

2.4.2 Water and Oil Condition and Setup of the Plates

For the water absorption experiments, a constant temperature water bath equipped with a sealing lid was supplied and placed on a table. It was filled with distilled water, and the lid was always kept closed to avoid the entrance of impurities and contaminants into the water. The constant temperature was set to room temperature (25 °C) for the first experiment, and 40 °C for all other experiments. A spiral stand was installed in the bath, as shown in Figure 2-6, and samples were

located between the spirals with a minimum contact with the stand. Silicone rubber plates were also immersed in a bath of 40 °C MotoMaster 2-Cycle Engine Oil.
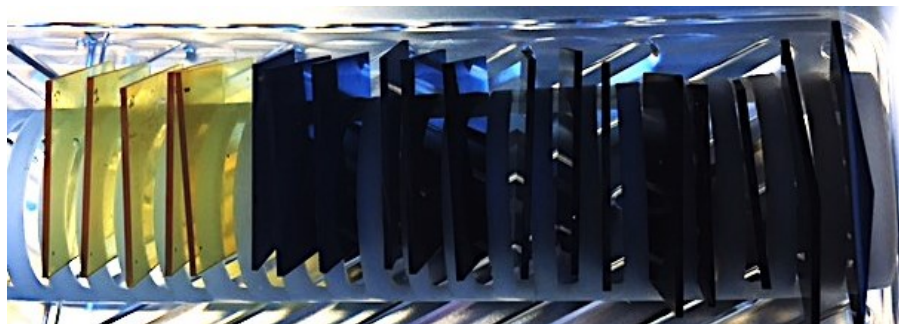
Figure 2-6 Setup of the spiral stand and sample plates in the water bath

2.4.3 Time Intervals

Different time intervals were defined to do the measurements in accordance with the pace of water absorption in the samples. As was mentioned in the literature, the water uptake of the material follows Fickian upward trend. Meaning that initially, there is a linear increase of the water uptake versus the square root of time, followed by a more gradual and non-linear increase as they get close to saturation. Therefore, smaller time intervals, i.e. 4-12 hours, were chosen at the beginning of the immersion, and as they became less sensitive to the changes of water uptake, the time intervals were extended, i.e. 24 hours- 1 week. At each time interval, plates were taken out of water, wiped gently with lint-free tissues, and the measurements were proceeded.

For the silicone rubber plates, the measurements were carried out following the same procedures as for epoxies, with the exception of having shorter time intervals, since the absorption was considerably faster for silicone rubber compared to epoxy. After taking the plates out of the oil bath, and before measuring their properties, all the extra oil was removed from their surface and

edges using lint-free tissues soaked with ethanol. Consistency was ensured throughout the whole experiment.

For the desorption experiments, saturated plates were taken out of water and wiped dry. Plates conditioned at room temperature, were placed in a room temperature desiccator cabinet, and the plates saturated in 40 °C water, were situated in an oven at 40 °C to desiccate the absorbed water. The time intervals to measure the properties of the desorbing samples followed a similar pattern to that of the absorbing stage, i.e. faster at the beginning and extending as the desorption slowed down. As the weight gain reduction reached a stabilized stage and no considerable change was noticed, all the plates were placed in an oven at 110°C for 24 hours and were completely dried.

2.5 Measurements and Observations

The sample plates were prepared and immersed into water. The objective of the experiment was to detect and explain the changes in certain properties of the nanocomposite with the absorption of water. At each time interval of both absorption and desorption procedures, samples were individually taken out of water or oven, and for the absorption, wiped dry with lint-free tissues until no visible moisture was observed on the surface and the edges. Afterwards, their weight, thickness, and electrical resistivity were measured, and calculations were carried out to obtain data including water uptake, diffusivity, and changes in electrical resistivity. SEM observations and T_g measurements were also conducted as additional quality control tests. All the measurement procedures and calculations will be described in details in the following subsections.

2.5.1 Water Uptake and Diffusivity

The absorption of water at each time interval was calculated by measuring the weight of the plates, and placing the values in Eq. 1.1. The average of water uptake of five samples with the same MWCNT concentration was obtained as well. The water uptake values were plotted against the square root of time as a means to observe the flow of water absorption.

Diffusivity values were also calculated using Eqs. 1.2 and 1.3, using the slope of the linear section of each water uptake versus square root of time graph.

2.5.2 Thickness

To measure the thickness of the samples, a calliper was installed on a fixed stand to minimize the operating errors. For a strong precision, nine points were designated on the surface of each plate, and the thickness of each point was measured and recorded at all time intervals. The thicknesses of the plates were defined by the average of these constant nine points for electrical resistivity calculations.

2.5.3 Electrical Resistivity

The practiced method to measure the electrical resistivity of the plates was the Van Der Pauw method, a commonly used technique for measuring the electrical resistivity of plate-shaped conductive materials. The next section provides a theoretical explanation of this method.

2.5.3.1 Van Der Pauw Method

Van der Pauw method is an electrical resistivity and Hall coefficient measuring system, applicable to semi-conductor materials with arbitrary two-dimensional shapes, i.e. thickness much smaller

than width and length. The plates, as demonstrated in Figure 2-7, should have uniform thickness and no holes [45,46].
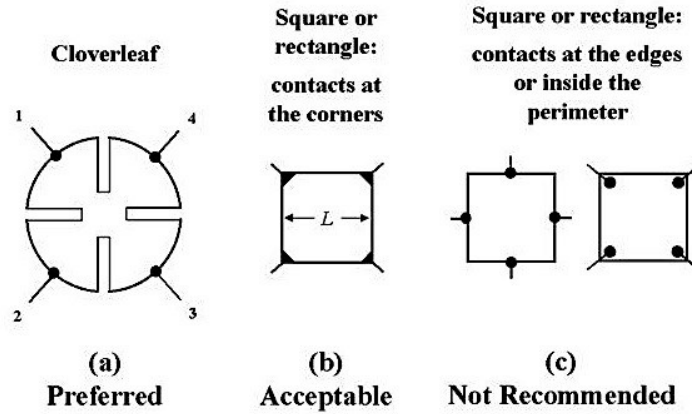
Figure 2-7 Desired shape of samples for Van der Pauw method [45].

Current source Keithky 6220 DC, and nanovoltmeter Keithly 218A were utilized. The setup, as shown in Figure 2-8, contains four probes that connect to the four corners of the plate with minimum contacts. Current is passed through one edge, points 1 and 2, and the voltage is measured at the parallel edge, points 3 and 4. The probes are then shifted 90 degrees, and with the same current passing through the adjacent edge, the second voltage is measured. The process continues until four voltages are achieved, and having the current and thickness, and using the Van Der Pauw equations as shown below, electrical resistivity is calculated (Eqs. 2.5- 2.8) [19,45,46].
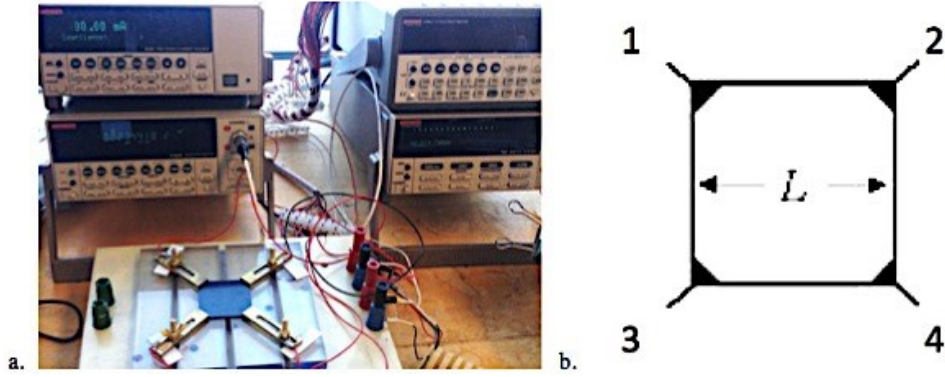
Figure 2-8 a) Resistivity measurement assembly, and b) schematic of a plate and four probes [45].

$$R_{12,34} = \frac{V_4 - V_3}{I_{12}} \qquad (2.5)$$

where $R_{12,34}$ is the electrical resistance obtained, with current passing through points 1 and 2, and voltage measured through points 3 and 4.

$$R_{vertical} = \frac{R_{12,34} + R_{34,12}}{2} \qquad (2.6)$$

$$R_{horizontal} = \frac{R_{23,41} + R_{41,23}}{2} \qquad (2.7)$$

$R_{vertical}$ and $R_{horizontal}$ are the averages calculated for the vertical and horizontal edges, respectively. The electrical resistivity is obtained using the following equation:

$$\exp\left(-\frac{\pi t}{\rho} R_{horizontal}\right) + \exp\left(-\frac{\pi t}{\rho} R_{vertical}\right) = 1 \qquad (2.8)$$

where t is the thickness of the plate and ρ is the resistivity.

2.5.4 Glass Transition Temperature (T_g)

The Glass Transition Temperature (T_g) of the nanocomposite before immersion and after saturation was measured by DSC TA Q10. The changes in T_g correlate with the structural changes occurred in the material, and show the extent of plasticisation caused by the reactions between the

water molecules and the epoxy. There were two objectives for measuring T_g; to see the influence of water absorption on T_g, and to see the influence of MWCNT content on T_g. The former was obtained by comparing the T_g of the plates in the dry and saturated conditions, and the latter was achieved by measuring the T_g of the neat epoxy as well as for the samples with 0.3, 0.5, and 1 wt.% MWCNT.

2.5.5 Scanning Electron Microscopy (SEM)

The Scanning Electron Microscope (SEM) presents an enlarged surface image of the samples by scanning the surface with an electron beam in vacuum. When the sample is exposed to the radiation of an electron beam, secondary electrons and backscattered electrons are generated to form images. The Secondary electrons near the sample surface, produce an SE image and reflect the fine topographical structure of the sample. Backscattered electrons reflect the composition and distribution of atoms on the sample surface.

In this research HITACHI SEM S-3400 was used to provide a clear image of the surface composition of the plates at their cross section, with magnification of up to 4.5K. Samples with different CNT concentrations were prepared and investigated to ensure that the amount of voids in each sample is less than 1 percent. The preparation of the samples and the observation procedure is briefly explained in the following subsections.

2.5.5.1 Sample Preparation

Prior to placing the samples in the vacuum chamber for the SEM observation, several steps have to be taken to prepare their surface, such as filing, polishing, and metal coating.

For each of the CNT concentrations, two samples with dimensions of 1x3 cm were cut and trimmed. All six samples, as shown in Figure 2-9, were placed in an aluminum stand and fastened together with screws in a way that their cross section was available for the SEM observation. The cross section of the plates was filed and polished with disk-like sand papers and polishing pads at 0 and 90 degrees using an orbit sander.
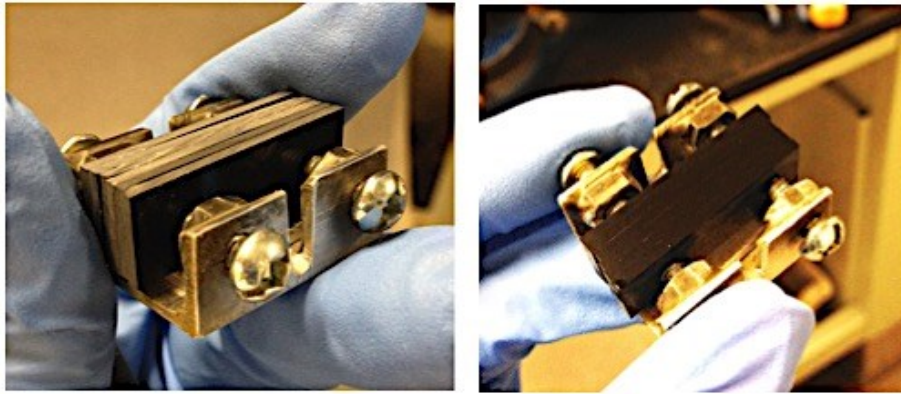
Figure 2-9 Setup of the plates for SEM observation a) before, and b) after surface filing and polishing

Tables 2-6 and 2-7 represent the steps of filing and polishing, respectively. Optical microscopy was done after each level of filing to assure the elimination of obvious scratch lines.

Table 2-6 Procedure of filing sample surfaces

Level	Sand papers (grits)	Time (min)
1	240	< 1
2	400	≈ 1
3	600	≈ 1
4	800	≈ 1-2

Table 2-7 Procedure of polishing sample surfaces

Level	Polishing pads (microns)	Time (min)
5	9	≈ 2
6	3	≈ 2-3
7	1	> 3

After the filing and polishing procedures, the surface of the samples was coated with a conductive metal layer. This step was done to make the sample surface conductive in order to prevent charge-up and damage to the sample, and also to increase the production rate of secondary electrons and image information. The sample setup was placed in a metal coating chamber, the air was pumped out and once the vacuum was obtained, the surface of the plates' cross section was exposed to platinum-palladium for 40 seconds.

2.5.5.2   SEM Observation

The prepared setup of the six samples was mounted on a stub using conductive tape. After adjusting the height, the specimen chamber of HITACHI SEM S-3400 instrument was closed, air was evacuated, current was passed, and the images were seen through the SEM software. The image results are shown in Chapter 3.

3 Results and Discussions

3.1 Absorption

3.1.1 Introduction

A number of plate-shaped samples were made with CNT reinforced epoxy nanocomposite. Different contents of Carbon nanotubes were used to obtain a wide range of conductivities. In addition, to obtain less variability in the conductivity of plates having the same nanotube content, two different types of Carbon nanotubes from two suppliers were used. Also, changes in material preparation processes contributed to a better dispersion of nanotubes in epoxy, and as a result, a higher conductivity was obtained. Furthermore, two different temperatures of 25 (room temperature) and 40 °C were used and different water absorption rates were obtained. An effort was also made to enhance the swelling of epoxy by modifying the degree of cure of the samples. Finally, a comparative analysis of epoxies and silicone rubber were performed to observe more clearly and efficiently the influence of swelling and volume change on the resistivity obtained by nanotubes.

The procedures and modifications introduced above were performed in seven individual absorption and two desorption experiments for the entire research. The water uptake, thickness change, and electrical resistivity results are illustrated in graphs and explained in details in the following sections.

3.1.2 SEM Observation

The image results of SEM observation are shown in Figure 3-1. Two plates of each MWCNT concentration were chosen and observed by SEM. As can be seen from these images, there are no evident defects on the surface of the cross sections, and the void content is less than 1%. The optimized procedure of three-roll milling and vacuum mixing led to the excellent dispersion of nanotubes and strong prevention of air voids inside the material.
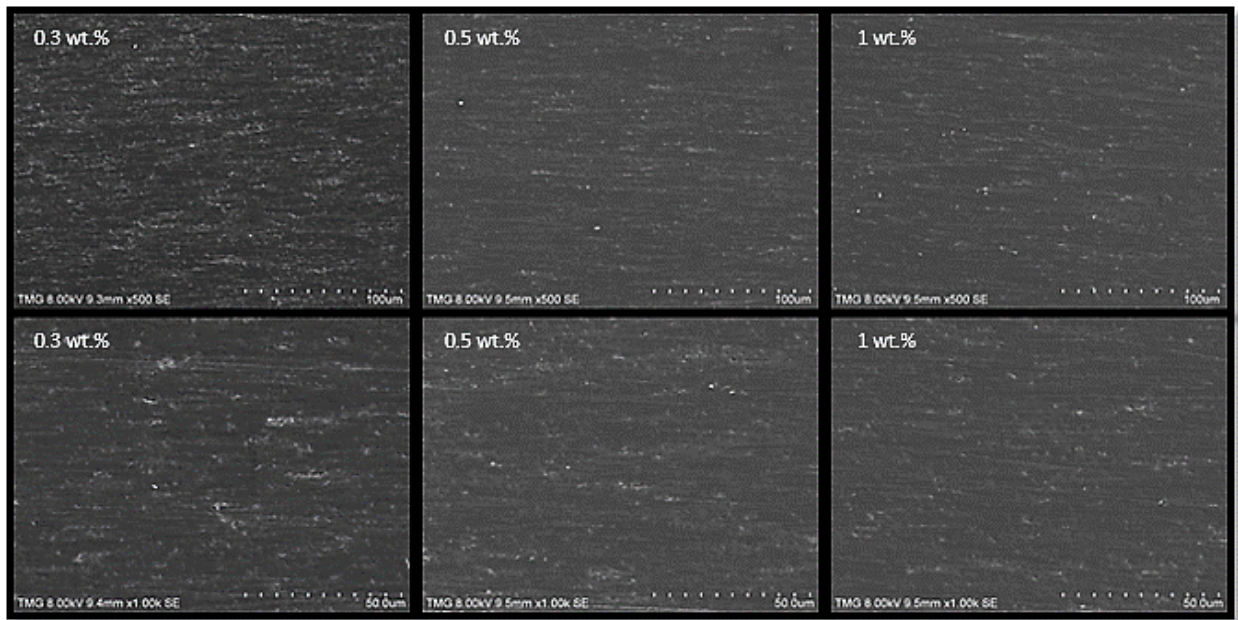
Figure 3-1 SEM images of plates containing 0.3 (left), 0.5 (center), and 1 (right) wt.% CNT.

3.1.3 Water Uptake and Diffusivity

The water uptake of the plates at each time interval was defined by the difference between the measured weight and the initial weight divided by the initial weight. The average water uptake of five plates was calculated for each CNT concentration and was plotted against the square root of time. Figure 3-2 shows the water uptake of C150P MWCNT reinforced nanocomposite plates immersed in room temperature water. It can be seen from the curve that the water uptake follows

a linear upward trend until approximately 1.5% weight gain, and gradually falls into a nonlinear increase, as plates get closer to reaching their saturation. This course of movement is in accordance with Fick's first law of diffusion. It has been previously shown that at low temperature immersions, up to 75 °C, water uptake in epoxies agrees with Fick's law [2,40]. It can also be concluded that all epoxy plates reached their saturation at around 2%.
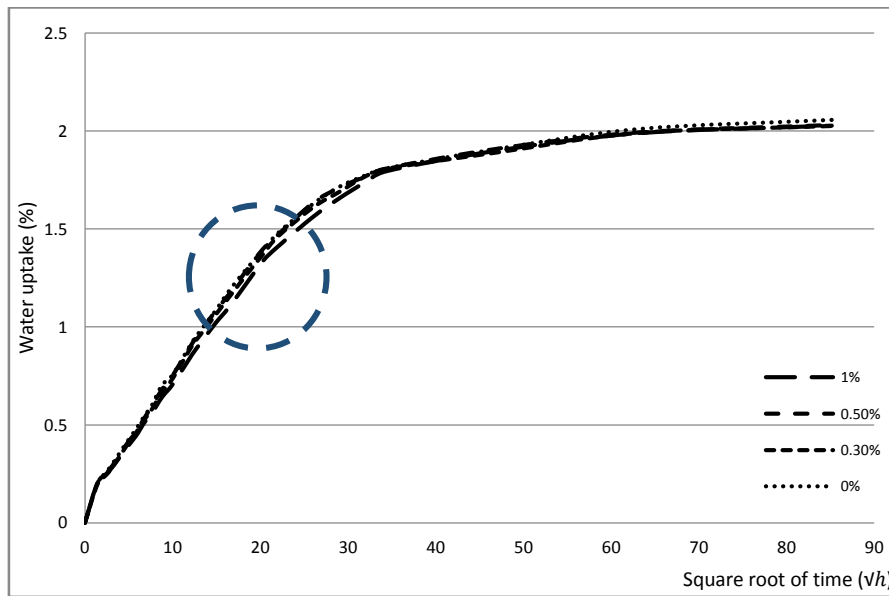
Figure 3-2 Average water uptake of plates with 0, 0.3, 0.5, and 1 wt.% C150P MWCNT immersed in room temperature water (the dotted circle is magnified in Figure 3-3).

Furthermore, the curve shows that CNT content does not have an influence on the level of saturation of epoxy nanocomposites, and regardless of the crowd of carbon nanotubes, the epoxy will reach its water saturation at around 2%. However, there was proved to be a difference in the rate of water uptake before saturation depending on the amount of nanotube occupying the plate, which is shown more clearly in Figure 3-3. According to this figure, the highest rate of water uptake goes to plates with 0.5 wt.% MWCNT, and the lowest rate is accounted for plates with 1 wt.% MWCNT, namely the highest MWCNT content. The plates with 0.3 wt.% or the smallest

content of MWCNT, have a rate of water uptake more than that of 1 wt.% and less than 0.5 wt.%. This phenomenon can be explained by considering two theories. On one hand, carbon nanotubes have hydroxyl groups on their surface, and attract water molecules due to the tendency to form hydrogen bonds. Therefore, they encourage water molecules to enter the samples at a higher rate, and the more the MWCNT content in the batch, the faster water is absorbed inside the sample. On the other hand, MWCNTs can act as barriers and limit the movement of water molecules into the plates. When there is a higher crowd of nanotubes, the distance between the nanotubes is less, and the barrier effect becomes more pronounced. Water molecules cannot move around easily, and hence the diffusion rate is decreased.

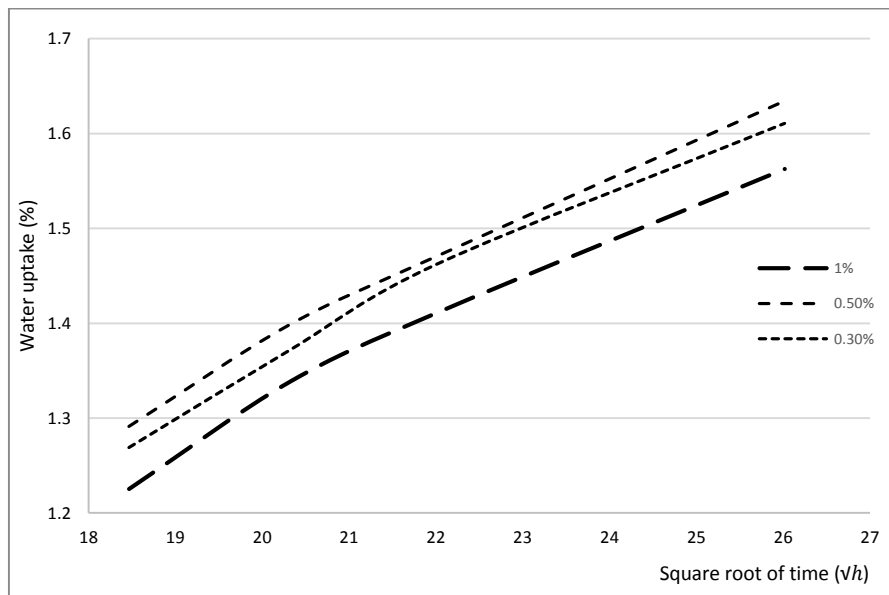Figure 3-3 Average water uptake of plates with 0.3, 0.5, and 1 wt.% CNT at room temperature (magnified section taken from figure 3-2).

Bearing in mind the two mentioned theories, one can conclude that for the case of 0.5 wt.% MWCNT, there is a higher number of CNTs in the material compared to 0.3 wt.%, and this leads to a stronger attraction of water molecules inside the samples before saturation. On the other hand,

the crowd of carbon nanotubes in 1 wt.% samples is twice as high as the 0.5 wt.%. Therefore, the barrier effect becomes more significant and dominates the movement of water molecules resulting in a slower water uptake inside the samples. Diffusivity values were obtained using the linear section of the curve of water uptake, and Eqs. 1.2 and 1.3, and are shown in Table 3-1.

Table 3-1 Diffusivity values for plates with neat epoxy and three CNT concentrations.

CNT Concentration (wt.%)	Diffusivity (mm²/sec)
1	1.280×10^{-7}
0.5	1.305×10^{-7}
0.3	1.285×10^{-7}
0	1.253×10^{-7}

Water uptake of C150P MWCNT reinforced nanocomposite plates immersed in 40 °C water was measured and plotted against the square root of time as shown in Figure 3-4.
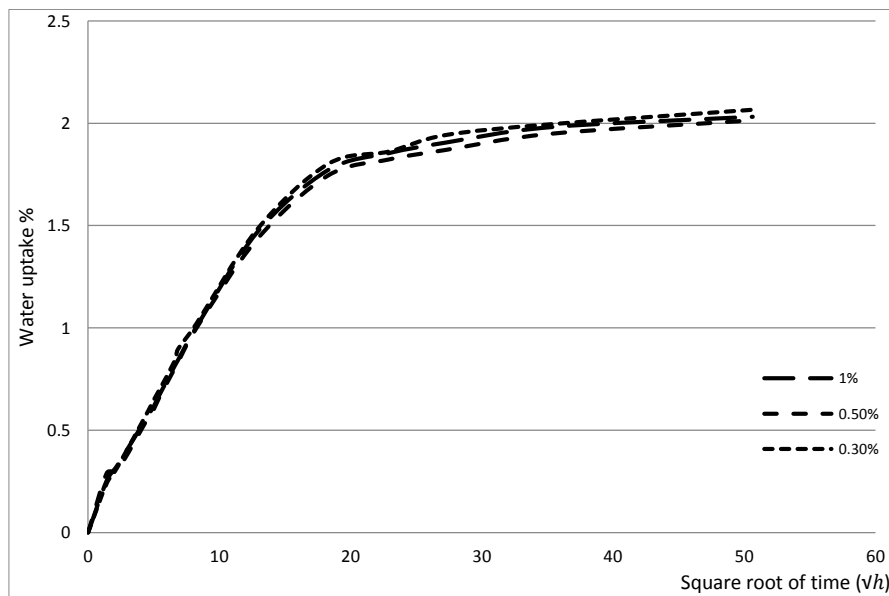
Figure 3-4 Average water uptake of plates with 0.3, 0.5, and 1 wt.% CNT immersed in 40 °C water.

The three charts in Figure 3-5 illustrate comparisons of water uptakes of the plates immersed in room temperature (25 °C) and 40 °C water for the three CNT concentrations. It is noticeable from

these figures that by raising the temperature of water, the absorption takes place faster and as a result, the saturations of the plates are reached in less time.
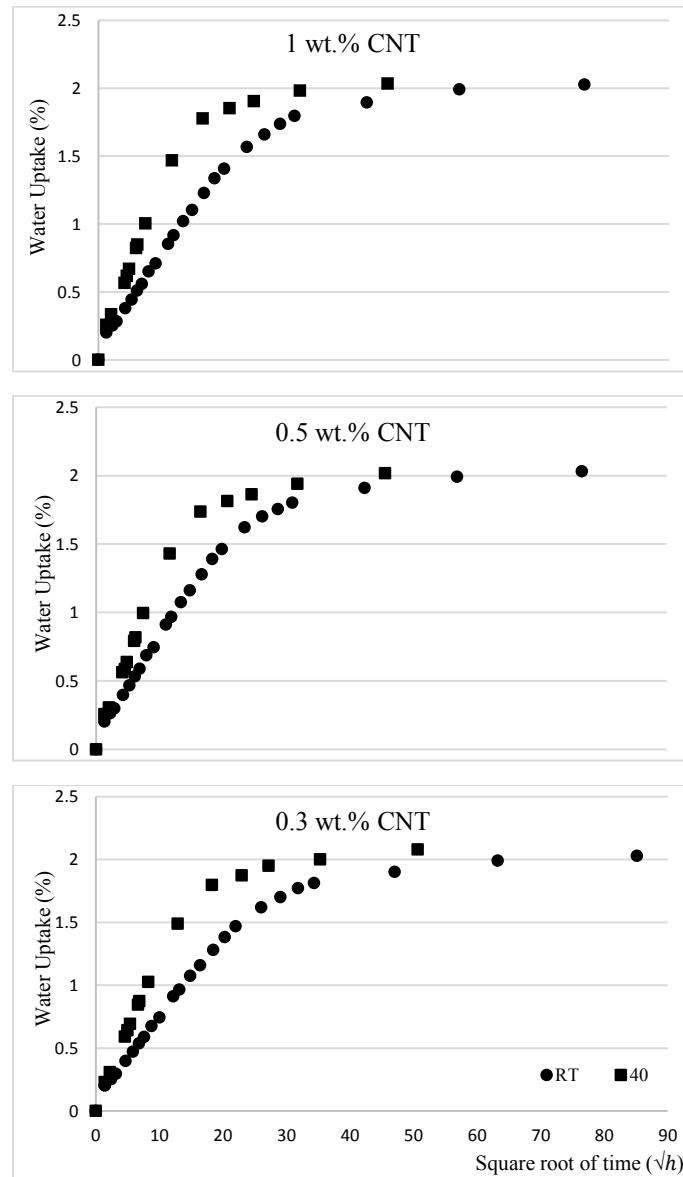
Figure 3-5 Comparison of water uptake of epoxy plates reinforced with 0.3, 0.5, and 1 wt.% C150P CNT immersed in room temperature water and in 40 °C water.

It is also evident from Figures 3-4 and 3-5 that for the case of this experiment, there exist two stages of linear and non-linear for the water uptake curves, which is in accordance with Fick's first

law of diffusion. Moreover, it is worth the mention that the level of saturation is the same and approximately 2% regardless of the temperature of water, even though the rate of water absorption is different from one CNT content to another.

With changing the type of carbon nanotube to IG MWCNT and immersing the plates in 40 °C water, it is shown in Figure 3-6 that the water uptake follows the same upward trend as with the previous type of carbon nanotube. The difference can be merely seen in the rate of water uptake before saturation, as illustrated in Figure 3-7, which is slightly lower than that of C150P MWCNT reinforced plates. It is explained by the aspect ratio and more specifically, the higher length of IG carbon nanotubes.
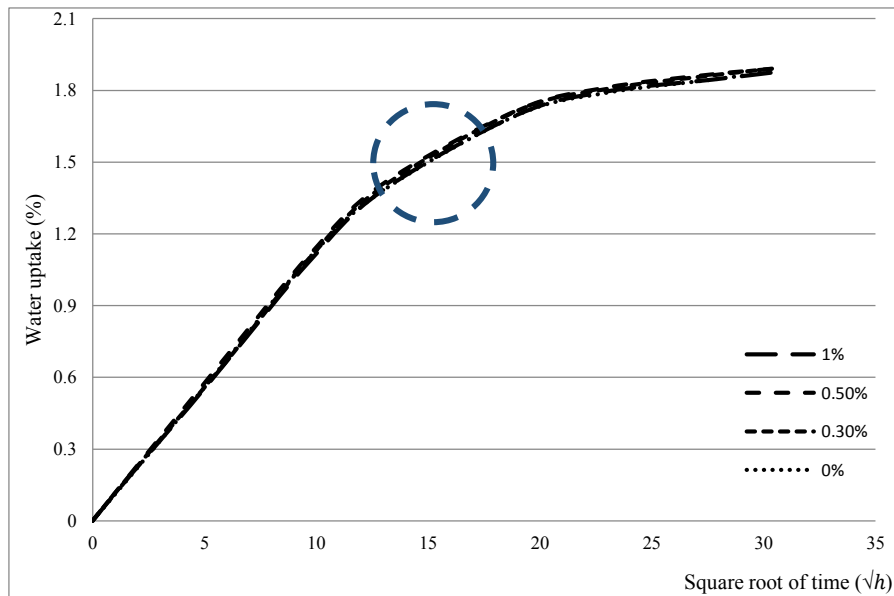

Figure 3-6 Average water uptake of plates with 0, 0.3, 0.5, and 1 wt.% IG MWCNT immersed in 40 °C water (the dotted circle is magnified in Figure 3-8).

The length, diameter, and aspect ratio of the two nanotubes were given in Table 2-3 of Chapter 2. According to this table, the average aspect ratio value of IG MWCNT is more than five times greater than that of C150P MWCNT, which leads to higher tortuosity of the diffusion path. Hence

the movement of water molecules struggling to diffuse deep in the material is restricted. In other words, there is a stronger barrier effect prohibiting the movement of water molecules.
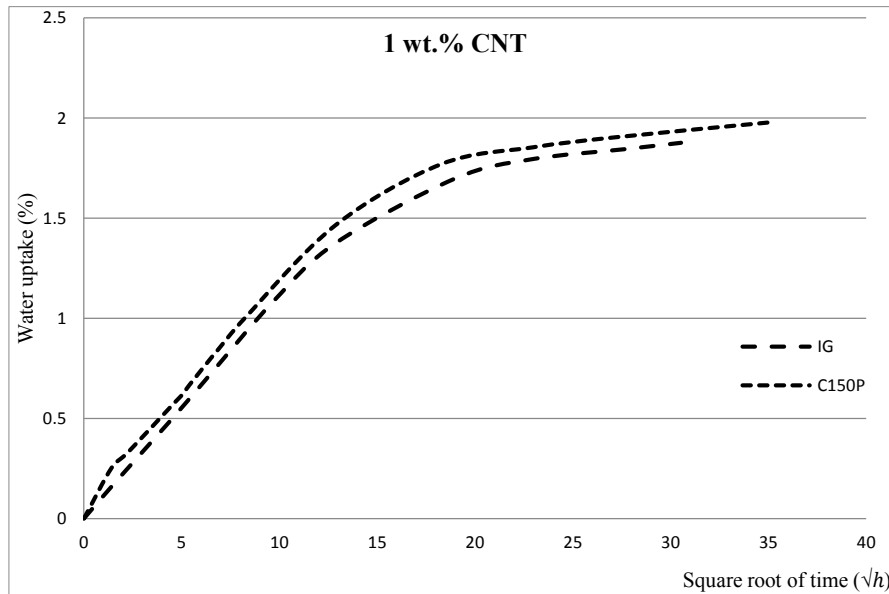
Figure 3-7 Comparison of water uptake of epoxy plates reinforced with 1 wt.% C150P and 1 wt.% IG MWCNT immersed in 40 °C water.

The diffusion behavior of plates with three different CNT concentrations is compared in Figure 3-8. The same pattern as for plates reinforced with C150P MWCNT was obtained.
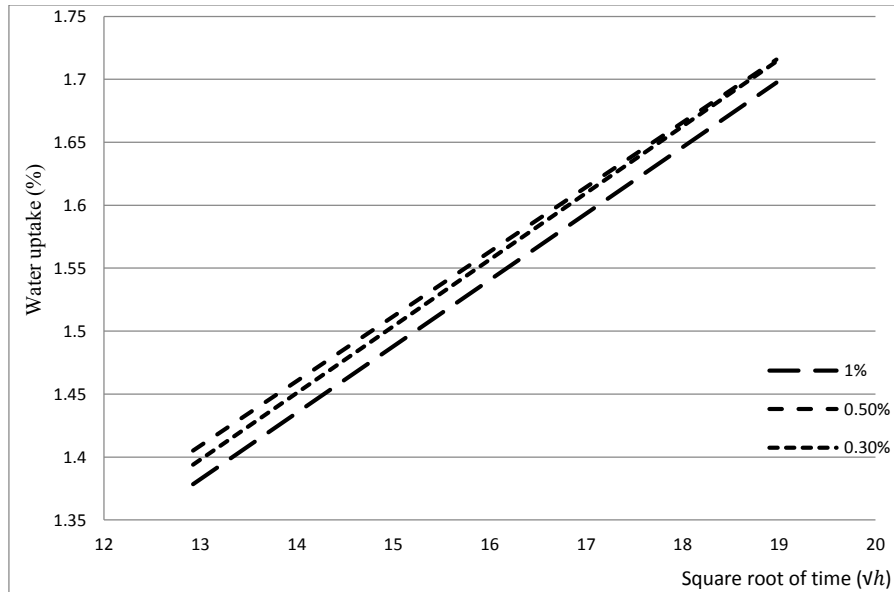
Figure 3-8 Average water uptake of plates with 0.3, 0.5, and 1 wt.% IG CNT immersed in 40 °C water (magnified section taken from figure 3-6)

The highest rate of water uptake goes to plates with 0.5 wt.% CNT, and the lowest rate is accounted for plates with 1 wt.% CNT. On one hand, carbon nanotubes attract water molecules by the polar functional groups on their surface, and form hydrogen bonds with them. On the other hand, more nanotubes in the material leads to a stronger barrier effect and prevents water molecules from entering the plates. One of the two becomes the dominant parameter affecting the rate of water absorption in the epoxy nanocomposite.

As explained in the Experimental Chapter, silicone rubber nanocomposite plates reinforced with IG MWCNT were fabricated and immersed in 40 °C engine oil. Saturation of silicone rubber nanocomposite with oil was reached in less than 24 hours for all CNT concentrations, as shown in Figure 3-9. A maximum weight gain of approximately 11% was obtained, which was more than 5 times the amount of water uptake in epoxies.
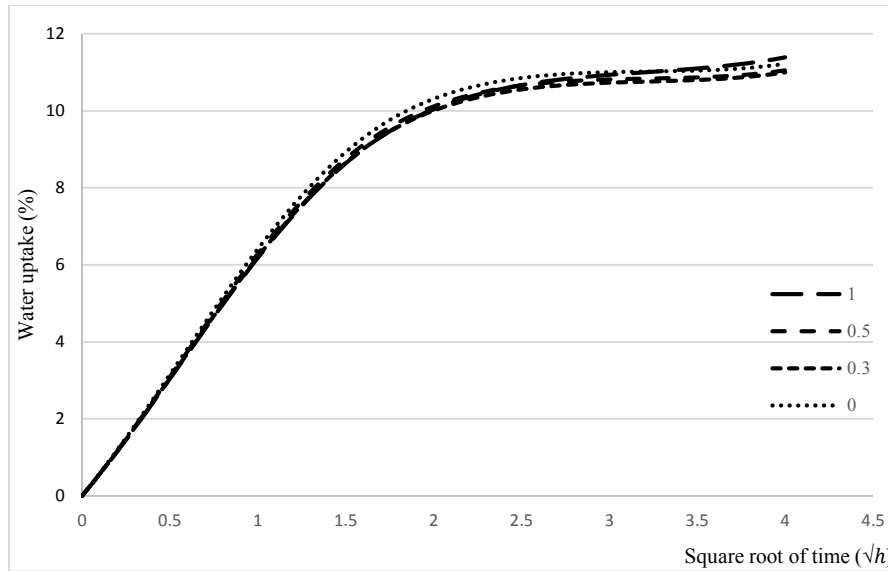
Figure 3-9 Average water uptake of silicone rubber plates with 0, 0.3, 0.5, and 1 wt.% IG MWCNT immersed in 40 °C engine oil.

3.1.4   Thickness

The thicknesses of nine points designated on the surface of each plate were measured and recorded.

Figures 3-10 to 3-15 show thickness changes of each point throughout the entire 40 °C immersion

procedure for plates containing 0.3, 0.5, and 1 wt.% IG and C150P MWCNT. As can be seen from

the figures, the thickness starts growing after a few hours of immersion, which indicates that water

diffuses inside the material and plasticizes the polymer chains resulting in the swelling of plates.

It has been shown in the literature that, whether epoxy is exposed to a humid environment or

immersed in water, it absorbs water, and the interaction between water and epoxy molecules

follows two different mechanisms [2,40].
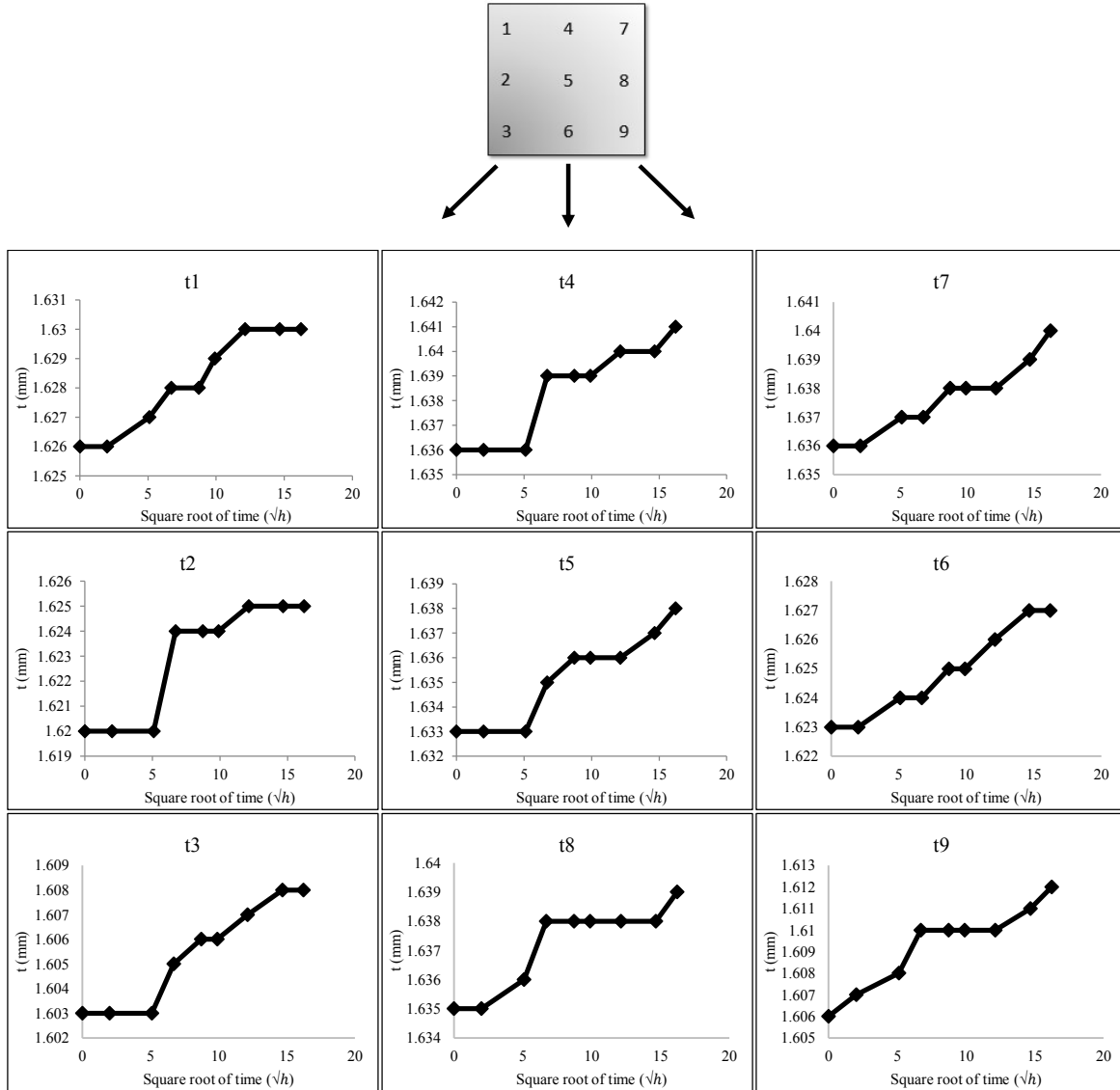
Figure 3-10 Thickness of nine designated points on epoxy plate 1 of 5 containing 1 wt.% IG MWCNT.

One mechanism supports the concept of free water, which fills up the free spaces inside the composite without forming any bonds. In the case of an epoxy containing MWCNT, this type of water accomplishes the same goal. It fills up the free spaces between the epoxy chains and carbon nanotubes, and does not react with the functional groups inside the material. Therefore, it shows no contribution to the changes in the dimensions of the plates. The second mechanism is ruled by so called bound water, which forms hydrogen bonds with the hydroxyl functional groups of

epoxies or N-H functional groups of amines. Bound water type I breaks Van der Waals forces between polymer chains and acts as a plasticizer. It increases the movement of polymer chains and eases the swelling of the material, and therefore, a change in the dimensions of the plates is detected.
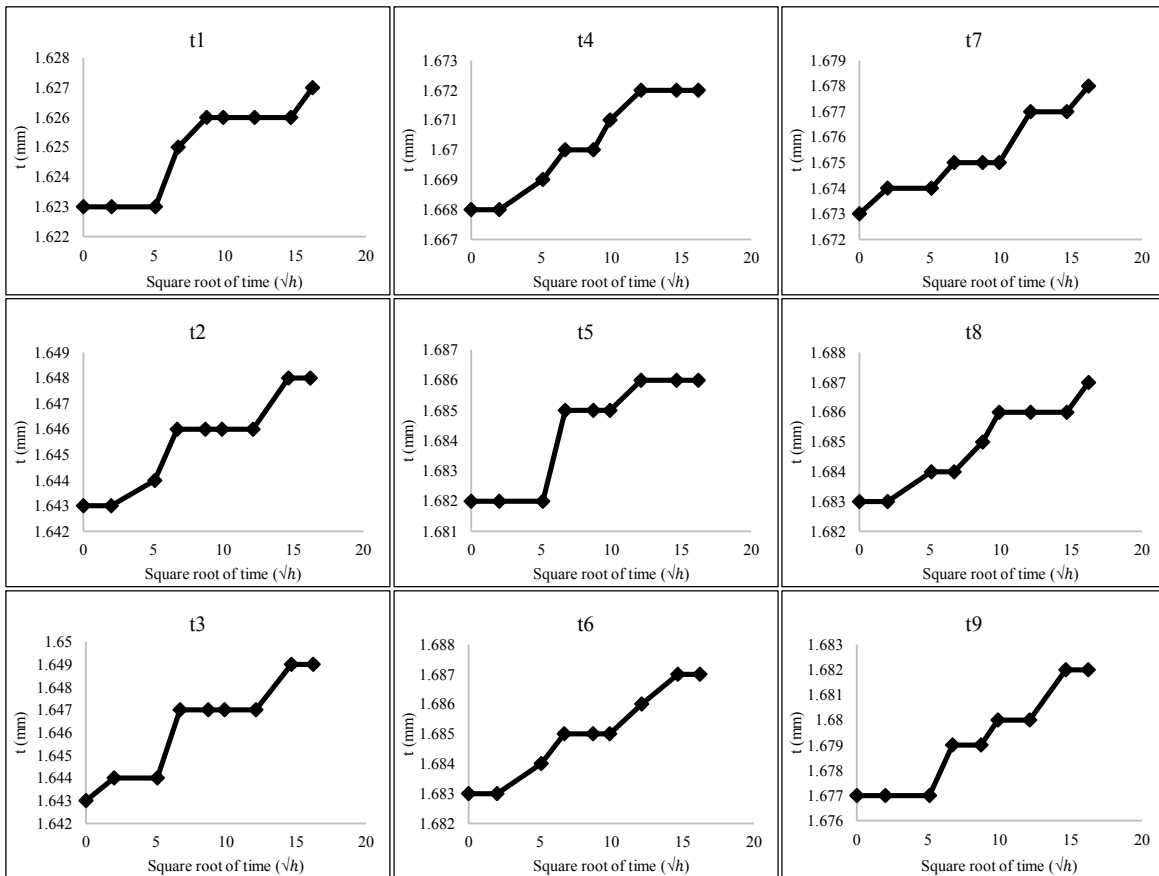
Figure 3-11 Thickness of nine designated points on epoxy plate 1 of 5 containing 0.5 wt.% IG MWCNT.

The average thickness change of IG MWCNT reinforced plates is slightly less than that of C150P MWCNT reinforced plates, 0.30% compared to 0.33%, which demonstrates the effect of nanotubes on swelling. The higher aspect ratio and entanglement of IG MWCNT prevents the material from separation to some extent.
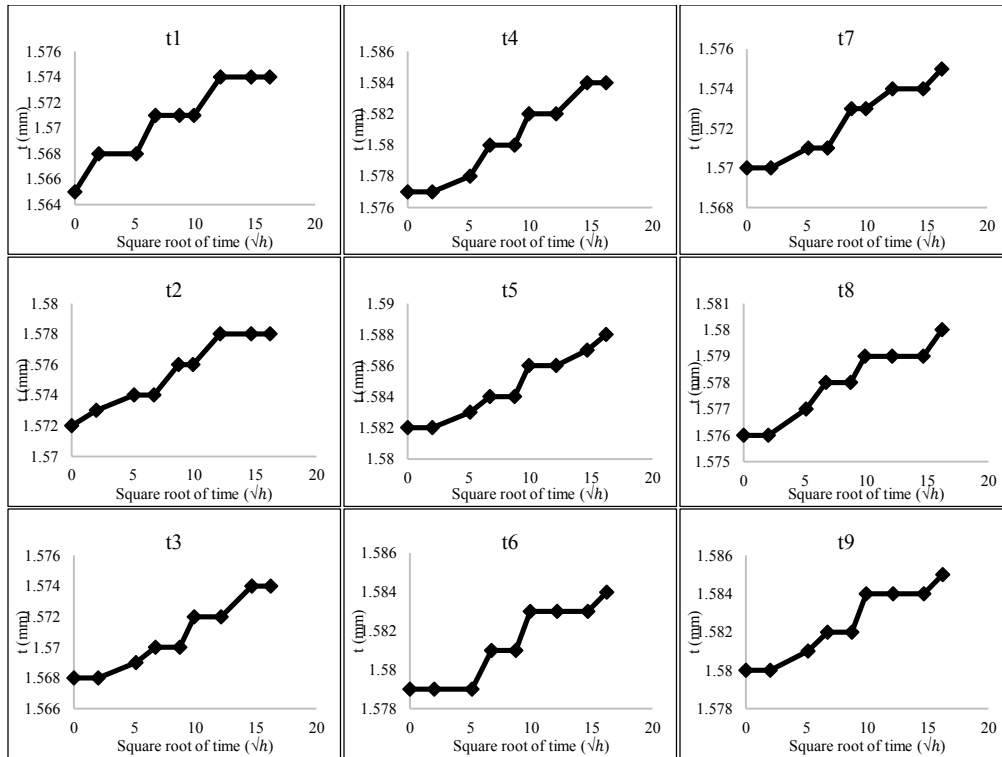
Figure 3-12 Thickness of nine designated points on epoxy plate 1 of 5 containing 0.3 wt.% IG MWCNT
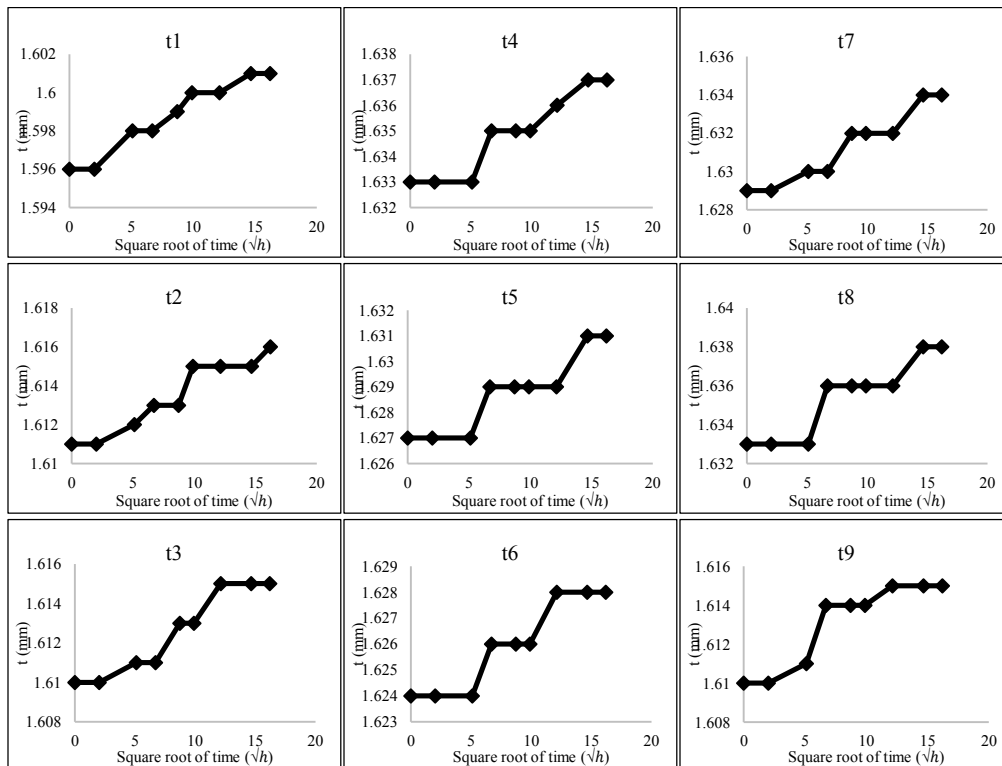
Figure 3-13 Thickness of nine designated points on epoxy plate 1 of 5 containing 1 wt.% C150P MWCNT.
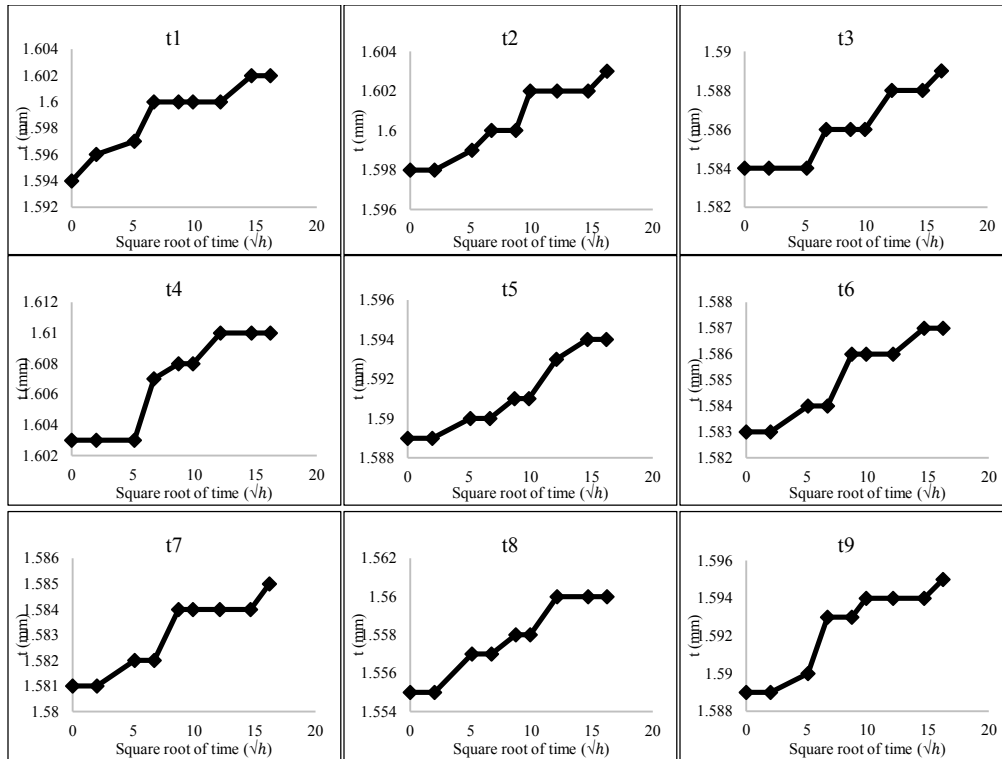
Figure 3-14 Thickness of nine designated points on epoxy plate 1 of 5 containing 0.5 wt.% C150P MWCNT.
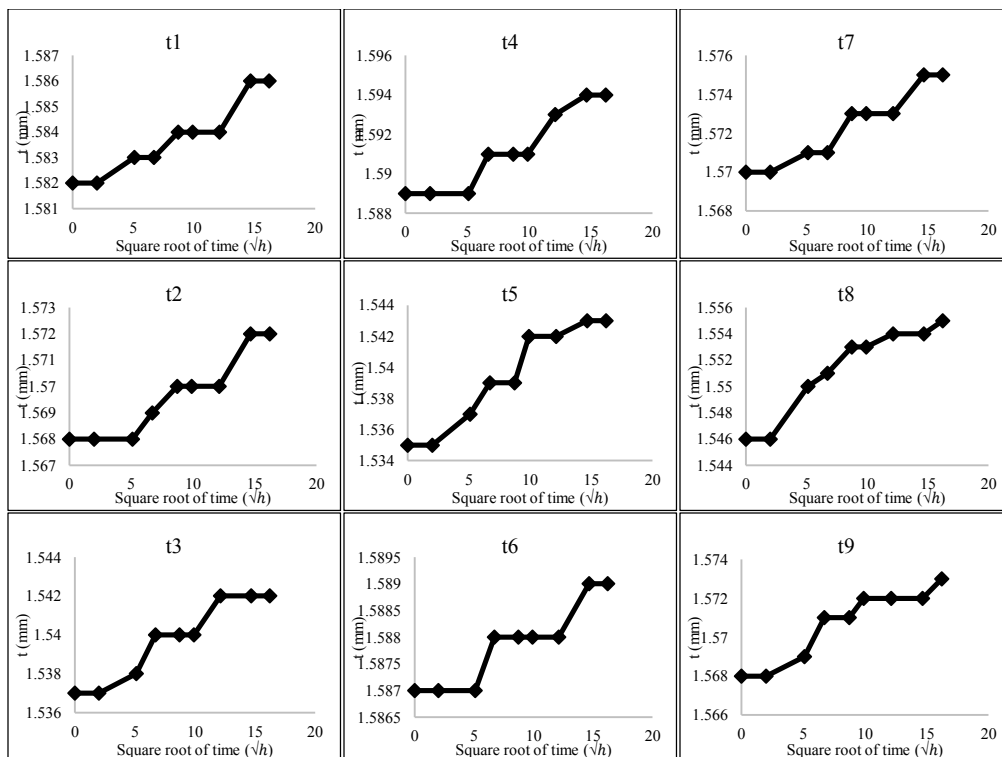
Figure 3-15 Thickness of nine designated points on epoxy plate 1 of 5 containing 0.3 wt.% C150P MWCNT.

The generalized trend of the thickness increases of the nine points on each plate was obtained through calculating the average value of nine points and was plotted as shown in Figure 3-16. As can be seen from this figure, the thickness change is slow at the beginning, due to the placement of free water in the material. The slow increase is followed by an inevitable increase of thickness detected for all points, which demonstrates the plasticizing effect of bound water type I. Then there is another gradual increase showing the gradual replacing of bound water type I by bound water type II.
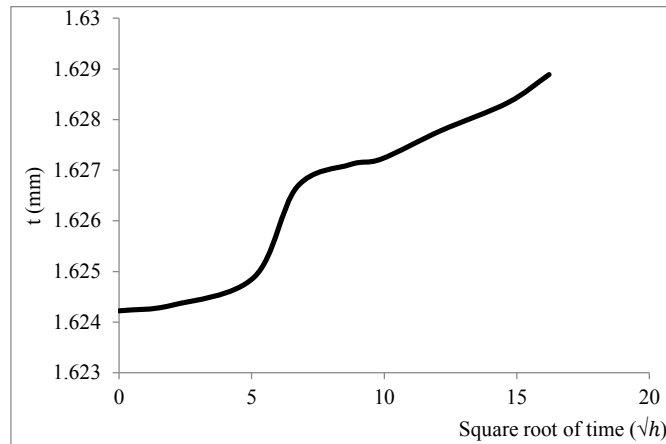
Figure 3-16 Average thickness of nine points on a 1 wt.% IG MWCNT reinforced epoxy plate.

For the case of silicone rubber immersed in engine oil, it was shown before that the plates gain up to 11% weight in less than 24 hours. In this short time compared to the saturation duration of epoxies, the thickness also increased up to twice the amount of epoxies, as illustrated in the graphs of Figure 3-17.
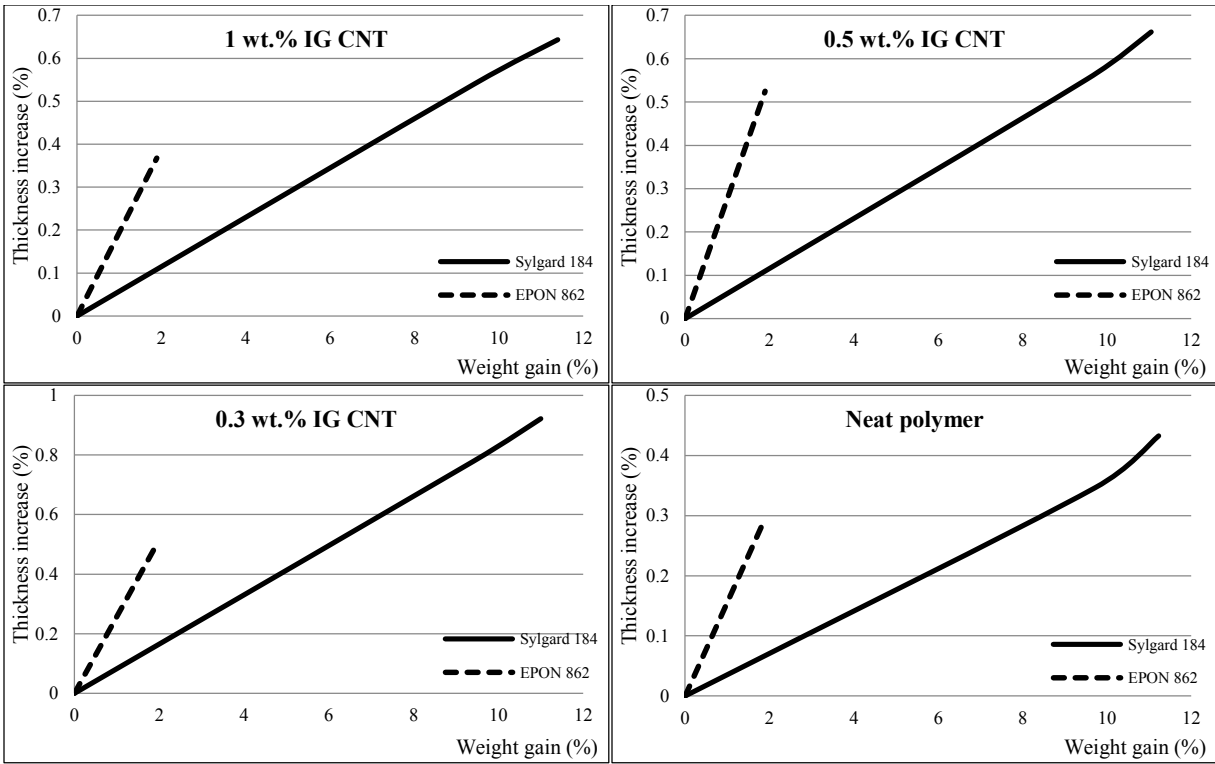
Figure 3-17 Comparison of thicknesses of epoxy and silicone rubber plates with 0, 0.3, 0.5, and 1 wt.% IG MWCNT

The figure shows the changes of thickness with weight gain. This immaculately illustrates the more pronounced extent of swelling of silicone rubber by absorbing engine oil. The oil plasticizes the SR polymer chains and diffuses among its networks resulting in the swelling of the nanocomposite.

3.1.5 Glass Transition Temperature (T_g)

Table 3-2 shows the glass transition temperature of 0, 0.3, 0.5, and 1 wt.% IG MWCNT reinforced plates, at dry and saturated conditions. According to this data, adding up to 1 wt.% MWCNT to the epoxy increases the initial T_g by 8 degrees, which is due to the strong entanglement of the nanotube networks.

Table 3-2 Glass transition temperature of IG MWCNT reinforced plates at dry and saturated conditions.

MWCNT Concentration (wt.%)	Glass Transition Temperature T_g (°C)	
	Dry	Saturated
1	136.1	123.1
0.5	135.8	122.2
0.3	134.4	119.2
0	128.4	107.6

It is also noticeable from the table that the addition of nanotubes results in a smaller drop of the T_g with water absorption. The T_g and the thickness data indicate that the existence of carbon nanotubes inside the nanocomposite weakens the plasticizing effect of water and decreases the movement of polymer chains. The non-reinforced plates showed a severe decrease of their T_g by approximately 21 degrees, whereas the reinforced plates showed 13-15 degrees decrease depending on their MWCNT content.

3.1.6   Electrical Resistivity

The electrical resistivity values at dry condition and each time interval were recorded for all the plates containing multi-walled carbon nanotubes. The range of resistivity for each MWCNT concentration of the C150P MWCNT reinforced plates is shown in Table 3-3.

Table 3-3 Resistivity values for plates with three C150P MWCNT concentrations.

CNT Content (wt.%)	Resistivity ρ (Ω.cm)
1	210-250
0.5	990-1500
0.3	6500-19000

It is easily noticeable that, as the content of CNT in the nanocomposites increases, the electrical conductivity improves, or better say, the electrical resistivity decreases. For the plates with 0.3 wt.% MWCNT there is a considerably wide range of resistivity among the five plates (6500-19000). This could be due to their CNT content being close to the percolation threshold of the carbon nanotube, which is 0.188 wt.%.

It can also be said that, carbon nanotubes due to their high polarity, have a tendency to attract each other and entangle. There is always a certain amount of MWCNT agglomerations randomly dispersed inside a batch of material, and this amount is considerably low for the case of 0.3 wt.% MWCNT. Since the five plates were made from the same batch, this random dispersion caused some plates to have more numbers of entanglements than others, which led to a difference in conductivity from one plate to another.

Throughout the entire room temperature immersion procedure of the nanocomposite plates, and as illustrated in Figure 3-18, the electrical resistivity of all samples was found to have an upward trend. In other words, water absorption caused the electrical resistivity of MWCNT-reinforced epoxy nanocomposites to increase. The absorption of water by the epoxy plates, leads bound water type I molecules to break Van der Waals forces and plasticize polymer chains. This phenomenon results in increasing the thickness, as it was shown in Figures 3-10 to 3-15.

Figure 3-18 Resistivity of nanocomposite plates reinforced with 0.3, 0.5, and 1 wt.% C150P MWCNT immersed in room temperature water.

Carbon nanotubes rest among polymer chains, and provide electrical conductivity throughout the plates by building conductive paths among each other. So, the swelling of polymer chains disintegrates carbon nanotube networks as well. Moving apart from each other, the conductive paths are elongated or in some cases completely lost, and this is seen as an increase in the electrical resistivity of the samples.

The changes in electrical resistivity is shown by $\Delta\rho\%$ and was plotted against the square root of time, as seen in Figure 3-19 for the average of five plates for each MWCNT content. It is noticeable

from the chart that, the overall percentage of increase in resistivity for samples with less amount of nanotube is higher.

Figure 3-19 Average electrical resistivity increase of five plates reinforced with 0.3, 0.5, and 1 wt.% C150P MWCNT immersed in room temperature water.

At saturation, the increase in electrical resistivity of 0.3 wt.% MWCNT plates is more than 2% higher compared to 1 wt.% MWCNT. That is to say, the electrical resistivity of the nanocomposite becomes more sensitive to water absorption and shows a more pronounced increase with the diffusion of water. This can be easily explained by the fact that, where there is lower MWCNT content, there exist fewer carbon nanotubes inside the material. Thus there are a limited number of conductive paths available, and the disconnection of one path will disturb the whole batch more severely.

The electrical resistivity of all C150P MWCNT reinforced plates immersed in 40 °C water, as shown in Figure 3-20, were also found to have an upward trend with water absorption.
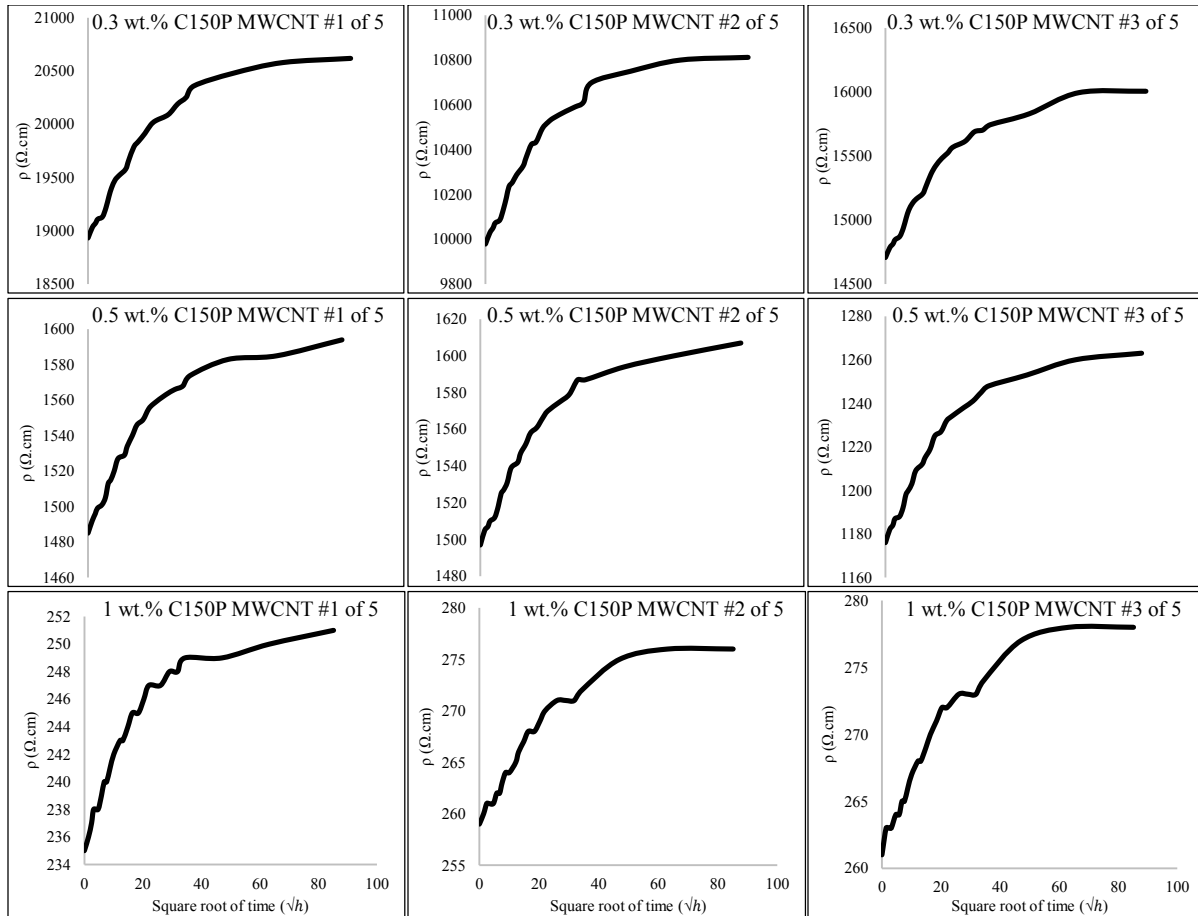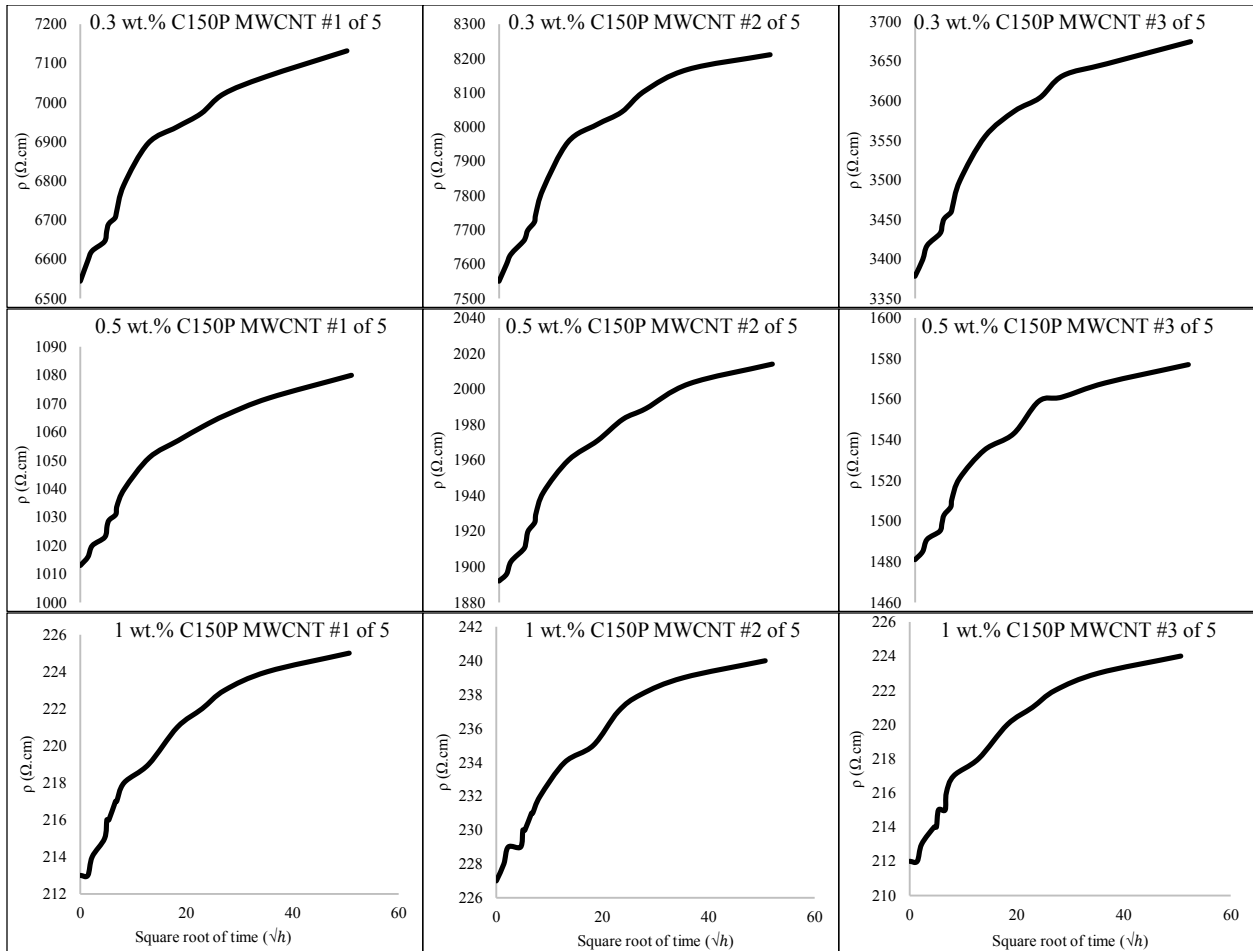
Figure 3-20 Resistivity of nanocomposite plates reinforced with 0.3, 0.5, and 1 wt.% C150P MWCNT immersed in 40 °C water.

The changes in electrical resistivity versus the square root of time for the C150P MWCNT reinforced plates immersed in 40 °C water were plotted as illustrated in Figure 3-21. The same trend as for plates immersed in room temperature water is followed by 40 °C water, demonstrating that plates with less MWCNT content show more enhancement in electrical resistivity by absorbing water.
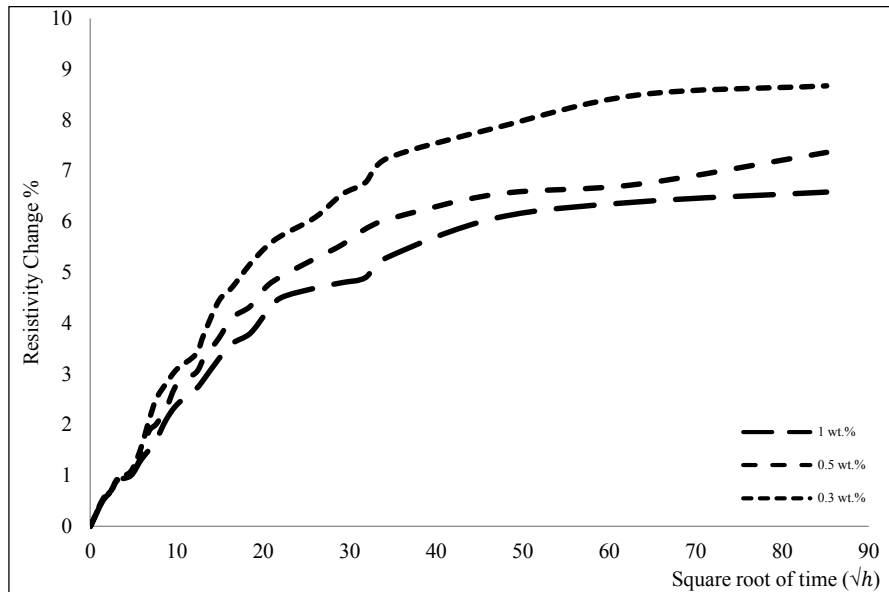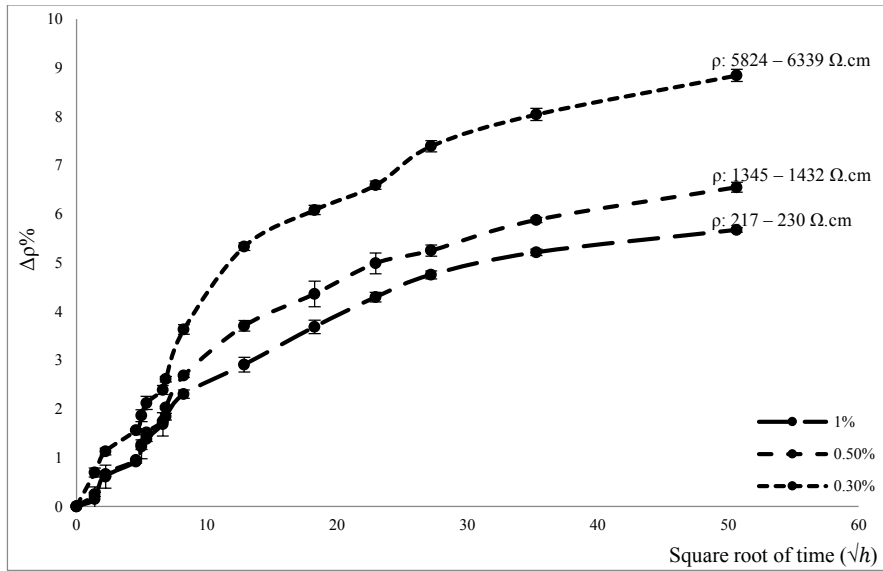
Figure 3-21 Average of electrical resistivity increase of plates with 0.3, 0.5, and 1 wt.% C150P MWCNT immersed in 40 °C water (each point has five replicates).

To investigate the effect of MWCNT type and aspect ratio on the electrical resistivity behaviour of the nanocomposite plates, a set of experiments were conducted using IG MWCNT reinforced nanocomposite plates. Table 2-3 in the Experimental Chapter demonstrated the properties of two types of carbon nanotubes utilized in this research. The information about length and diameter of each nanotube was provided by its supplier and re-measured by Rosca and Hoa [24], and their aspect ratio along with their percolation threshold were measured by Rosca and Hoa [24]. It can be maintained from the table that the aspect ratio of IG MWCNT is more than five times greater than the C150P MWCNT, leading to a higher tortuosity and more entanglement of the nanotubes. Therefore, a higher number of conductive paths per CNT content exist, and the fifteen-time smaller percolation threshold is a result of this configuration of nanotubes. Figure 3-22 illustrates the increase in electrical resistivity of IG MWCNT reinforced plates with the square root of immersion time. The trend is in accordance with the C150P MWCNT reinforced plates, indicating that less

content of MWCNT makes the nanocomposite more sensitive to the changes of electrical resistivity with absorption of water.
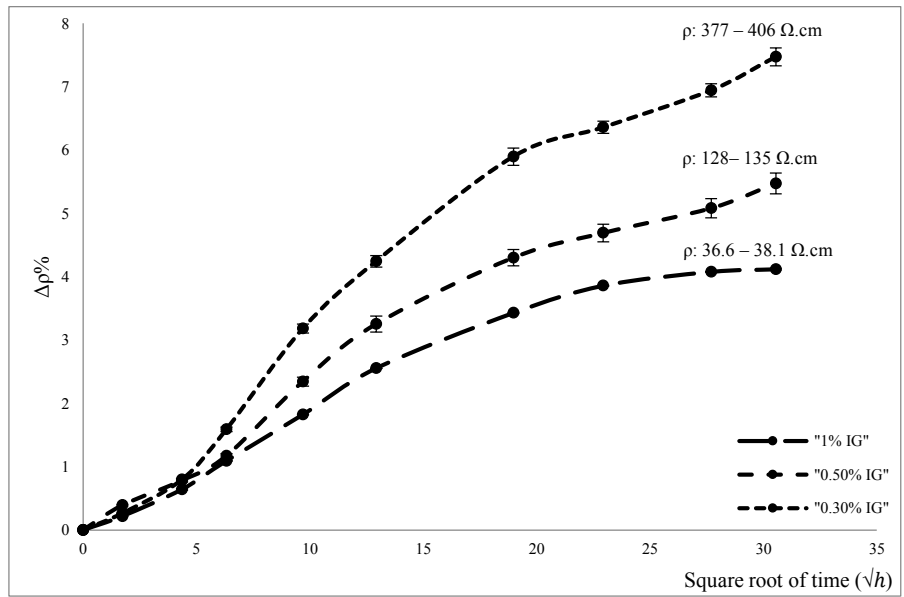
Figure 3-22 Average electrical resistivity increase of plates reinforced with 0.3, 0.5, and 1 wt.% IG MWCNT immersed in 40 °C water (each point has five replicates).

Figure 3-23 compares two plates reinforced with 1 wt.% MWCNT, one with C150P and the other with IG MWCNTs.
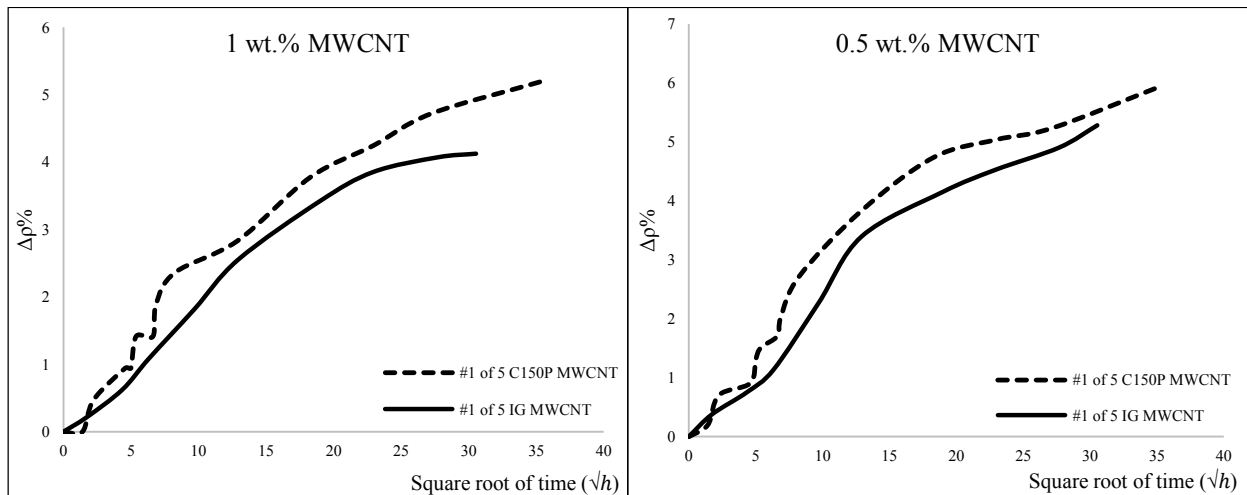
Figure 3-23 Comparison of electrical resistivity increase of epoxy plates reinforced with 1 wt.% C150P CNT and 1 wt.% IG MWCNT immersed in 40 °C water.

The difference between the two MWCNTs is noticeable through a lower and more stabilized elevation of electrical resistivity for the IG reinforced plates. This is due to the improved agglomeration of nanotubes as a result of their higher aspect ratio, which makes them more persistent against the swelling effect of water.

The significant difference between C150P and IG MWCNT reinforced plates became evident with the measurement of the electrical resistivity of the plates. More than 80% reduction in the initial electrical resistivity was obtained by merely changing the nanotube type. Table 3-4 shows the range of electrical resistivity of the plates containing 0.3, 0.5, and 1 wt.% C150P and IG MWCNTs.

Table 3-4 Comparison of electrical resistivity of plates reinforced with 0.3, 0.5, and 1 wt.% C150P and IG MWCNT.

CNT (wt.%)	ρ (Ω.cm)		Reduction (%)
	C150P	IG	
1	210-250	35-39	84
0.5	990-1500	125-143	90
0.3	6500-19000	370-430	97

By replacing C150P with IG MWCNT, not only plates with higher conductivity were achieved, but also the variability of resistivity was reduced from one plate to another, as illustrated in Figure 3-24, making properties of the plates more similar.
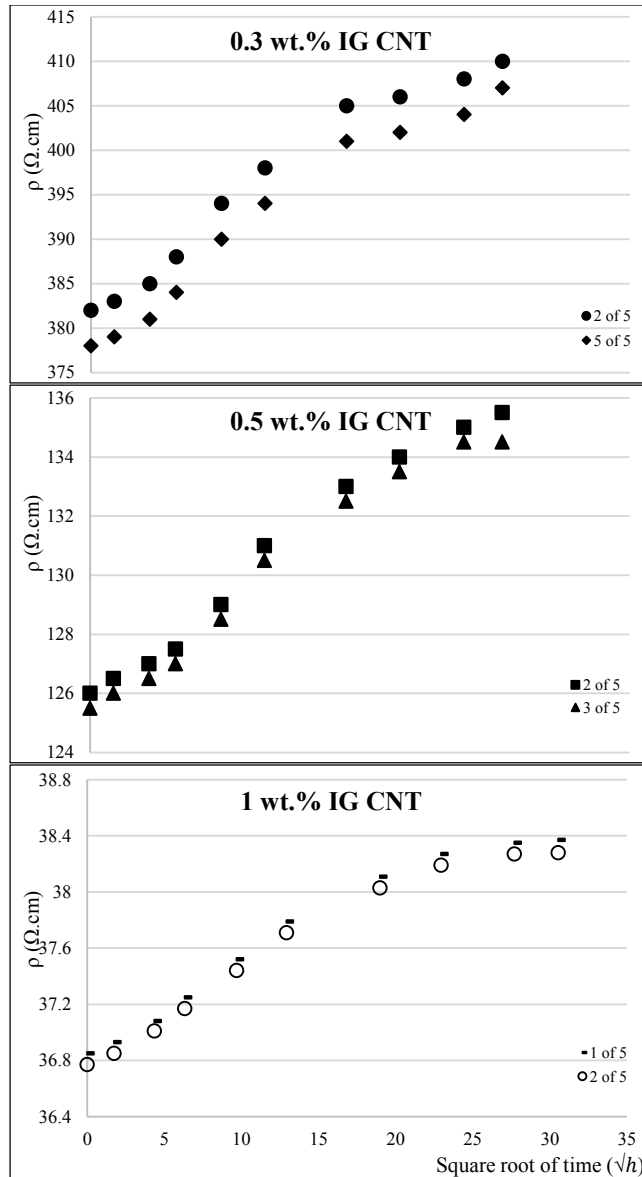
Figure 3-24 Electrical resistivity of plates with 0.3, 0.5, and 1 wt.% IG CNT immersed in 40 °C water.

After intensifying the swelling of plates by replacing epoxy with silicone rubber, and water with engine oil, electrical resistivity values were measured. Figure 3-25 shows the increase in electrical resistivity of silicone rubber with immersion time, whereas the change of electrical resistivity with the increase in thickness is demonstrated in Figure 3-26. A considerable growth of 900% for 0.5 wt.% IG MWCNT and 500% for 1 wt.% IG MWCNT plates were obtained for the electrical resistivity values. It is necessary to mention that, although 0.3 wt.% MWCNT plates exhibited a

resistivity of about 5000 ohm.cm before oil immersion, they did not show any signs of conductivity even after 3 hours of immersion.

There is a significant difference between 900% resistivity increase in silicone rubber and 5% resistivity increase in epoxy nanocomposite. Swelling plays an important role in this phenomenon. As discussed before, the plasticization effect of water molecules in epoxy plates causes the movement of polymer chains and results in restructuring and volume change of the plates.
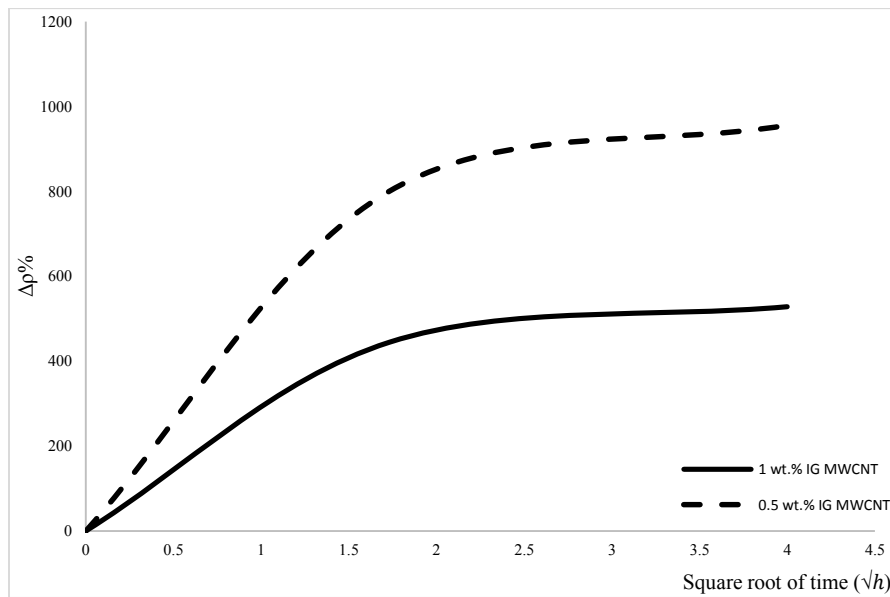
Figure 3-25 Electrical resistivity increase of silicone rubber plates with 0.5, and 1 wt.% IG MWCNT versus the square root of time immersed in 40 °C engine oil.

This volume change increases the distance between carbon nanotubes and thus, their conductive paths are elongated or in some cases disconnected, which is shown through an increase in the electrical resistivity of the nanocomposite. In the case of silicone rubber as well, the same mechanism is considered to be affecting the electrical resistivity. Swelling leads apart the elastomer chains and hence the nanotubes. However, this theory does not include an adequate

explanation of the increase of electrical resistivity to this extent, when the thickness has only increased twice the amount of epoxy.
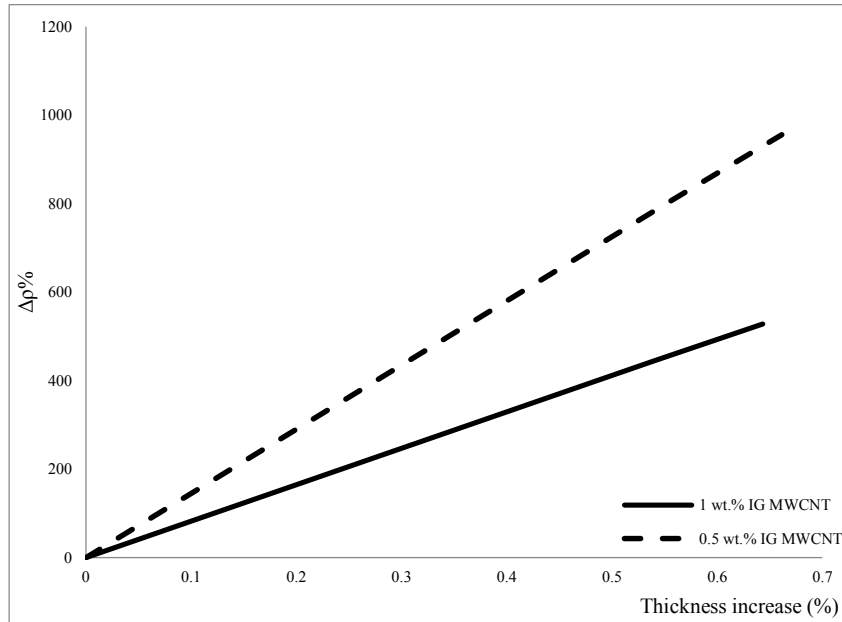
Figure 3-26 Electrical resistivity increase of plates with 0.5, and 1 wt.% IG CNT versus the increase of thickness immersed in 40 °C engine oil.

There is another factor strongly affecting the behaviour of carbon nanotubes towards swelling, and it is assumed to be time. By looking back to the water absorption of epoxy nanocomposites, it can easily be seen that for the case of epoxy, saturation was reached after 2500 hours of immersion, while it only took 24 hours for silicone rubber to absorb its full extent of oil. The distancing procedure of polymer chains in epoxy took place in an extremely slower manner. Carbon nanotubes were affected by the movement of polymer chains, but in a very gradual process, that made it possible for them to keep their entanglements. Although they were eventually separated to some degree after 0.5% thickness increase of the plates, they managed to resist the motion of polymer chains and were not forced to disentangle. This was not the case for silicone rubber plates. All the weight and thickness gain happened in less than 24 hours. SR polymer chains showed a strong tendency to separate from each other and let the engine oil diffuse inside the batch of

material, which directly influenced the movement of carbon nanotubes and caused their disentanglement, without providing any chance to resist disentanglement or regain their conductive paths. This fast-paced movement caused a complete disconnection of conductive paths in 0.3 wt.% IG MWCNT plates, as well as major disconnections in the 0.5 and 1 wt.% plates.

3.1.7 A Model for Electrical Resistivity Behavior of Epoxy Nanocomposites with Water Absorption

It was observed from the absorption results that the concentration of MWCNT in the material affects the diffusion of water. On one hand, carbon nanotubes attract water molecules by the polar functional groups on their surface, and form hydrogen bonds with them. On the other hand, high contents of MWCNTs act as barriers and slow down the diffusion of water inside the material. It was also seen that the electrical resistivity of MWCNT reinforced epoxy nanocomposites increases with water absorption, and composites containing smaller concentration of MWCNTs are more sensitive to water absorption; they show a more pronounced increase in their electrical resistivity due to the limited number of conductive paths between their MWCNTs. Moreover, higher aspect ratio of nanotubes slows down the water diffusion, due to the tortuosity of the diffusion path, and helps obtaining better entanglement, more conductive paths, and higher conductivity.

In order to better explain the transport of water from the surface through the thickness of the MWCNT reinforced epoxy nanocomposites, an electrical circuit consisting of three components connected in parallel is considered, the schematic of which is shown in Figure 3-27. The three parallel resistance combination demonstrates the surrounding of a nanotube-to-nanotube contact. Since there exist air, water, or both in the vicinity of the MWCNT conductive path, the

combination consists of the resistance of air (R_a), water (R_w), and nanotube joint (R_{CNT}) situated parallel from each other.
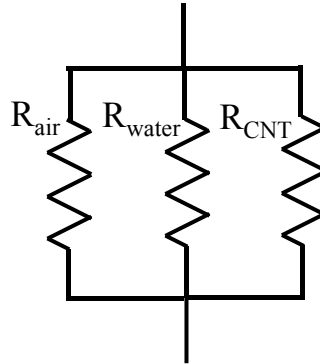
Figure 3-27 Schematic of three resistances surrounding a nanotube-to-nanotube contact

Table 3-5 shows the electrical resistivity of air, water, and IG MWCNT. At the dry condition, there exists only air surrounding a nanotube-to-nanotube contact among epoxy polymer chains, and since the electrical resistivity of air is considerably higher than the nanotube conductive path, the current will pass through this path. At the beginning of immersion, air is partially replaced by water. But again the electrical resistivity of water is much higher compared to nanotube contacts, and the current will pass through the nanotube conductive paths. As the immersion continues, water replaces the air in the material, and if one considers the mechanism of water transport only through the free water, this type of water will have no effect on the changes of electrical resistivity, since current only passes through the component with the smallest value of electrical resistivity.

Table 3-5 Electrical resistivity values of air, water, and IG MWCNT.

Component	Electrical Resistivity (Ω.cm)
Air	10^{18}
Distilled Water	10^{6}
IG MWCNT	10^{-3}

However, the results show that by absorbing water, the electrical resistivity increases. The type of water that demonstrates the difference between the role of water and air is bound water type I. It plasticizes the polymer chains and causes swelling and increase in thickness, as shown in Figures 3-10 to 3-15.

Figure 3-28 shows a schematic of the effect of thickness increase on the disconnection of carbon nanotube conductive paths. Swelling acts as a tensile force pulling carbon nanotubes apart from each other.
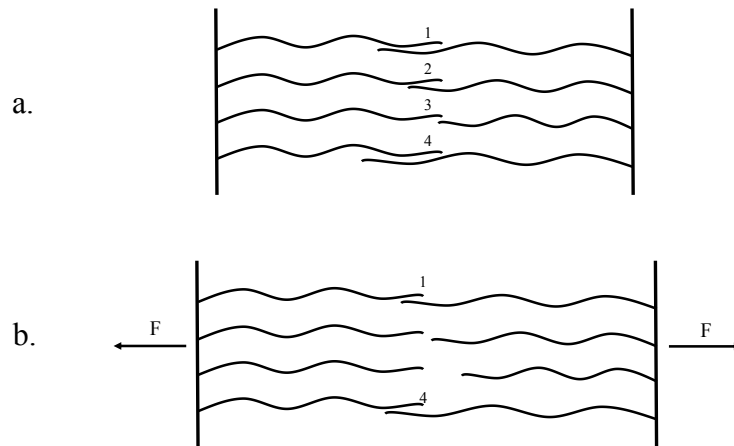
Figure 3-28 Schematic of the nanotube-to-nanotube joints a) before swelling, and b) after swelling.

This effect is better shown in Figure 3-29. The formation of hydrogen bonds plasticizes the polymer chains and separates them. Changes occurred in thickness lead to the restructuring of nanotube entanglements, and affect the functionality of conductive paths, by disconnecting or elongating the nanotube-to-nanotube joints.
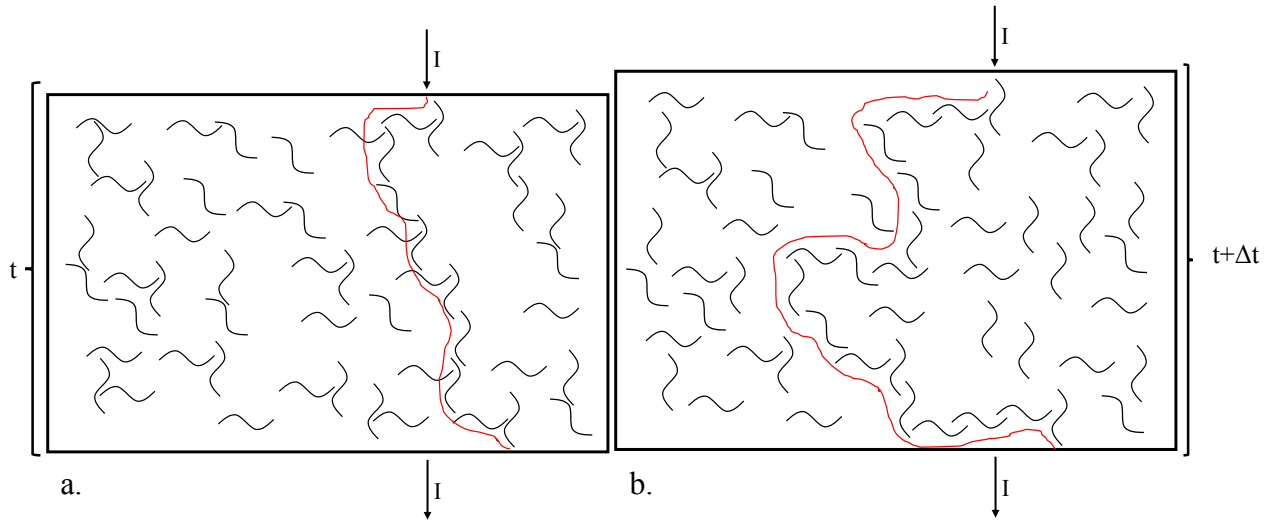
Figure 3-29 Schematic of the configuration of carbon nanotubes through the thickness of the plates a) before and b) after water absorption.

Nanotube-to-nanotube contacts are hypothetically located in n rows throughout the entire thickness, and the resistance of each row is located in series with the next row. The schematic of the electrical circuit of carbon nanotube networks is shown in Figure 3-30. When measuring electrical resistivity, current enters from a probe on the surface of the plate, and passes through the first row of conductive paths, through the component with the lowest electrical resistivity. Then it enters the second row, and again passes through the smallest value of the electrical resistivity. This procedure continues until the current passes through the whole thickness, and voltage data is obtained. The same mechanism can be considered for the width and the length of the plates.

When plates absorb water and their thickness increases, some of the nanotube networks are disconnected, and the entire conductive path is changed, as shown in Figure 3-31.
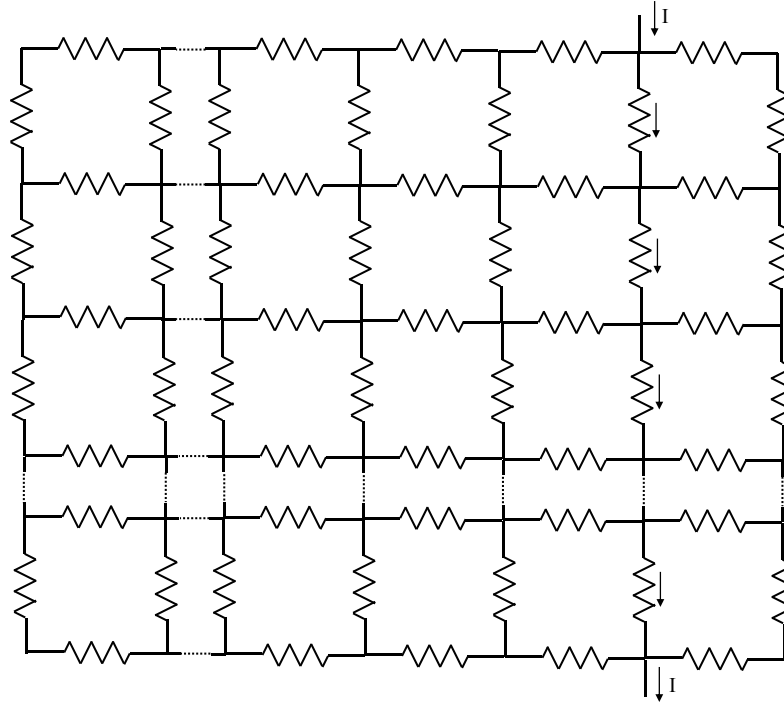
Figure 3-30 Schematic of the through-thickness electrical circuit before water absorption.
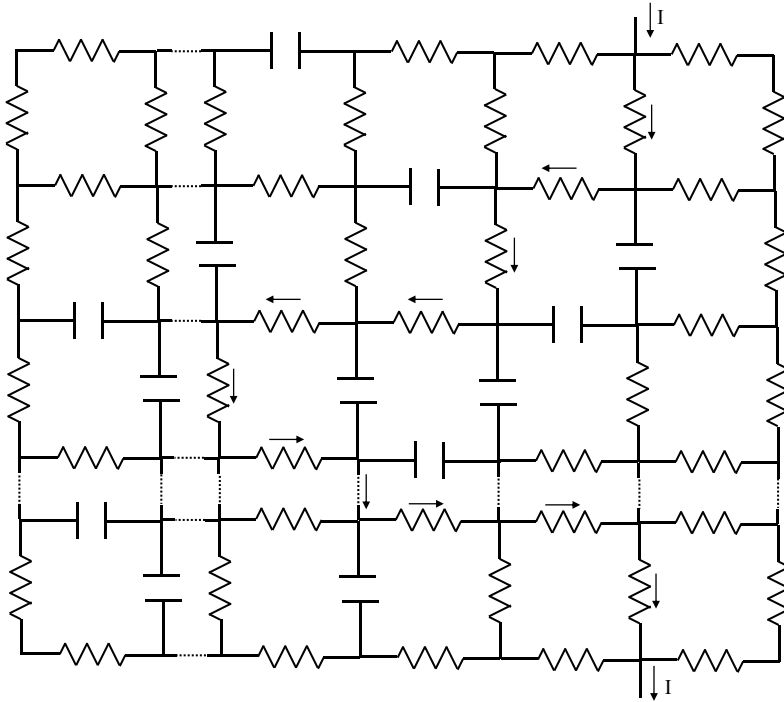
Figure 3-31 Schematic of the through-thickness electrical circuit after water absorption.

As previously mentioned in the literature, Barkoula et al. [23] investigated the effect of water absorption on the electrical resistance of CNT reinforced epoxy nanocomposites. They found that the absorption of water causes the electrical resistance to increase at the first 25 hours of immersion, and then decrease to values even less than their initial values. This was not the case for the results of this thesis, since a continuous increase of electrical resistivity with the absorption of water was observed. However no explanation of their results was provided. Since they measured the resistance through the length of the material, and did not provide the dimensions of their nanocomposite plates, the electrical resistivity values could not be obtained.

3.2 Desorption

3.2.1 Introduction

Carbon nanotube reinforced epoxy nanocomposites were immersed in water and several experiments were conducted. During the immersion, at different time intervals, measurements of weight, thickness, and electrical resistivity were carried out for each nanocomposite plate and data was recorded. Water uptake in the plates followed a Fickian upward trend, consisting of a linear section followed by a non-linear increase until the plates reached their saturation. With water absorption in the samples, increase in both thickness and electrical resistivity was observed. These two factors were explained to be correspondent with each other; swelling was considered to be the main cause for gaining electrical resistivity, and the transport of water inside the samples led to swelling. Therefore, it was speculated that by drying the nanocomposite and decreasing weight gain, electrical resistivity would be reduced. In order to investigate the recovery of the properties,

it was decided to conduct a desorption procedure for the nanocomposite. Two desorption experiments were performed simultaneously. The results are explained in details in the following sections.

3.2.2 Water Desorption

Figure 3-32 shows the decreasing trend of water uptake of both experiments for all MWCNT concentrations. It is easily noticeable that the nanocomposite loses its water more rapidly when placed in a higher temperature. The figure also exhibits a linear reduction of water uptake followed by a non-linear and more gradual stage of weight loss.
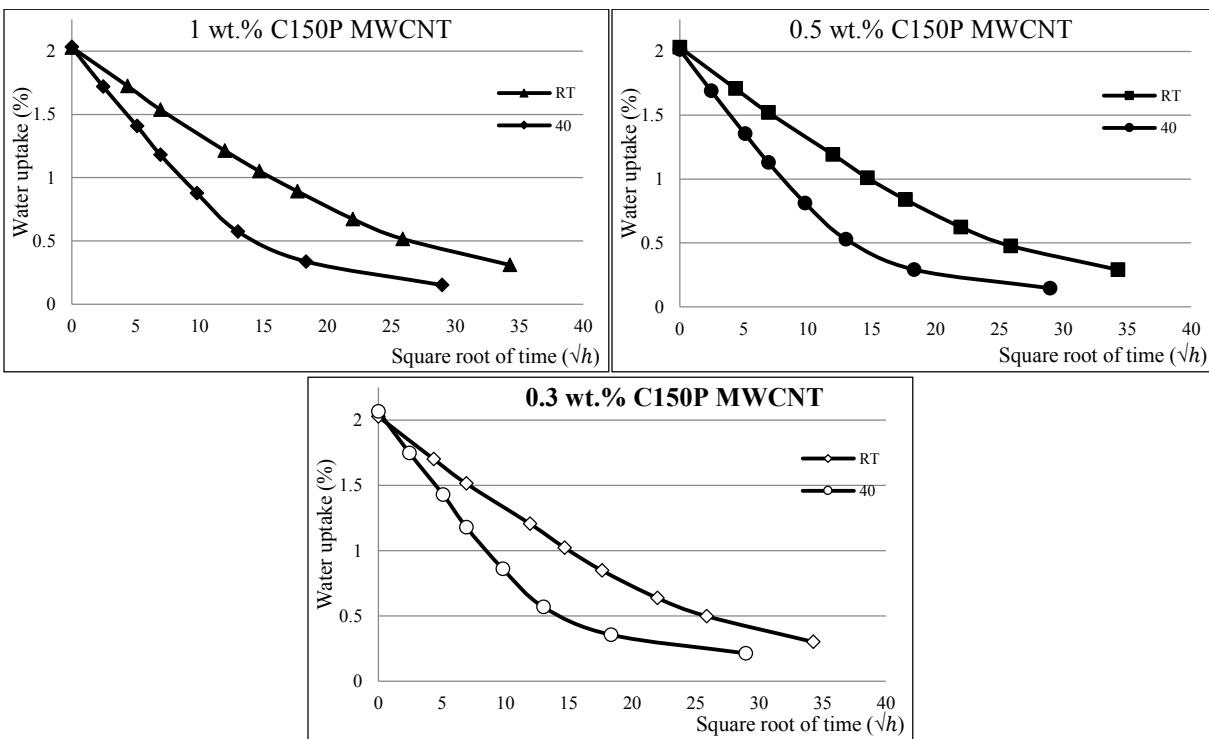
Figure 3-32 Comparison of water desorption of epoxy plates reinforced with 0.3, 0.5, and 1 wt.% C150P CNT in room temperature desiccator and 40 °C oven.

It can be seen in both cases that, the rate of weight loss lowered dramatically at 0.3% water uptake, showing that water molecules strongly resist exiting the material. This phenomenon is explained using the theory of water transport. Bearing in mind the mechanism of water entering and diffusing

inside the batch of material, it is assumed that there are three types of water. Free water goes inside the plate and simply fills up the empty spaces, with no influence on the structure of the material and no formation of bonds. It is easily removed from the material when the plates are taken out of the bath. This type of water mostly dominates the linear stage of the weight reduction, which shows a rapid loss of water mass in the plates. Bound water type I, is the kind of water that moves to the vicinity of epoxy polymer chains, breaks the Van der Waals forces, and forms a hydrogen bond with the OH- or NH- functional groups in the polymer chains. It acts as a plasticizer and causes the swelling of the material. Since there are hydrogen bonds formed with this water, it cannot be removed as effortlessly as free water. However, when the plates are placed in a dry environment, due to the equilibrium amount of water in the air, it eventually frees itself and comes out of the material. It explains the non-linear reduction of the weight gain during the desorption procedure. The 0.3% extra weight remaining in the samples shows that there is still water existing in the material, which is explained by bound water type II. This kind of bound water is considered to be transformed gradually from bound water type I. In a sense that, bound water type I forms only one hydrogen bond with the polymer, while type II forms two hydrogen bonds with two different parts of the cross-link, attaching forcefully to the material. As a result, it cannot be easily removed from the plates, and the activation energy equal to that of breaking two hydrogen bonds is needed to be able to detach this type of water. Therefore, the plates were placed in an oven at the elevated temperature of 110 °C to provide this level of energy and eventually, all the remaining water exited the material. Figure 3-33 illustrates the two stages of weight reduction for the epoxy plates reinforced with 1 wt.% C150P MWCNT.
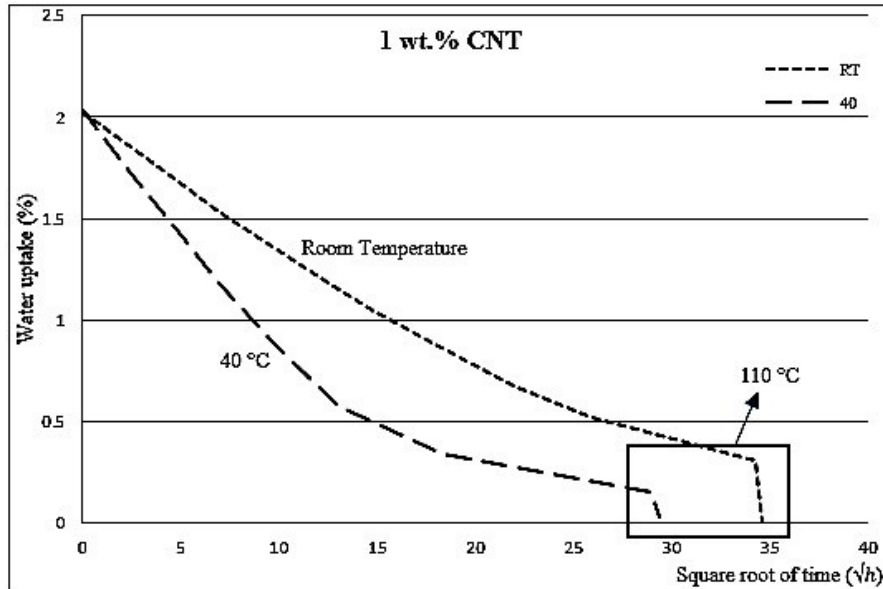
Figure 3-33 Two-stage water desorption of epoxy plates reinforced with 1 wt.% C150P CNT from Experiments One and Two, first at their absorption temperature, and second at 110 °C.

3.2.3   Electrical Resistivity

The electrical resistivity gain was plotted against the square root of time, as shown in Figure 3-34. The electrical resistivity of the plates dropped faster at 40 °C compared to room temperature, which is directly related to the higher rate of weight loss in those plates due to the elevated temperature. It can be seen from this figure that, after completely drying the plates, the electrical resistivity did not go back to its original value.
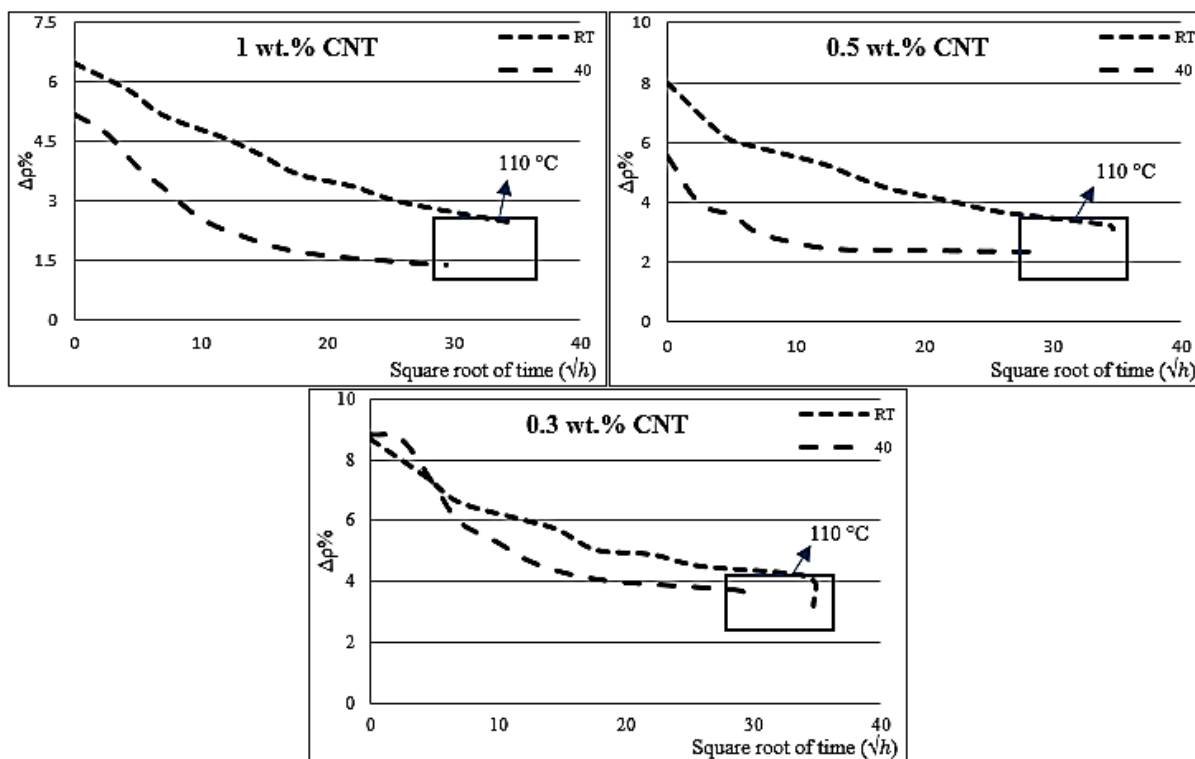
Figure 3-34 Electrical resistivity change of epoxy plates reinforced with 1 wt.% C150P CNT from Experiments One and Two during two-stage water desorption, first at their absorption temperature, and second at 110 °C.

Carbon nanotube conductive paths were elongated due to the swelling and restructuring of the polymer. The volume change led to the disconnection of some of the conductive paths, while others continued to pass the current. When the plates were dried, the expansion of the material was also recovered to some extent, helping carbon nanotubes reinforce or even regain some of their conductive paths. However, reorganizing of the polymer chains and restructuring of nanotube entanglements during absorption resulted in the loss of some of the conductive paths. After all, the electrical resistivity did not prove to be completely recoverable.

4 Conclusions and Recommendations for Future Works

4.1 Conclusions

Addition of carbon nanotubes to epoxies as multifunctional materials has enhanced the properties of these polymers and expanded their industries of demand. CNTs as nanoscale particles with large aspect ratios provide electrical conductivity and give epoxies the potential to be used in electronics industry and sensors for structural health monitoring techniques. However, one of the concerns of utilizing epoxy-based composites is its susceptibility against the absorption of water when exposed to humid environments. The transport of water into the material alters the functionality of carbon nanotubes as well and hence, the electrical conductivity is affected. The objective of this research was to investigate the mechanism of water transport inside the CNT reinforced epoxy nanocomposites, and the role of water absorption in altering the electrical resistivity of the material. For this purpose, plates were made with epoxy matrix and different kinds and contents of carbon nanotubes. They were immersed in water, and their water absorption and electrical properties were measured at different time intervals, until they reached saturation. The recovery of these properties were also studied through desorption experiments.

After comprehensive absorption experiments, it was concluded that water saturation in all plates, irrespective of the CNT content and the water temperature was reached at approximately 2% water uptake. The concentration of MWCNT in the material affected the diffusion of water. The polar functional groups in the structure of carbon nanotubes helped attract water molecules and formed hydrogen bonds with them on one hand, and on the other hand, more crowds of MWCNTs

prohibited the diffusion of water molecules inside the plates due to their barrier effects. Moreover, as the temperature of water increased from room temperature to 40 °C, the mobility and diffusivity of water molecules increased, and the saturation was reached in less time. The placement of water molecules inside the material resulted in the growth of the plates' thicknesses, which was used as a means of identifying the extent of swelling, and was in direct relation with the increase in weight gain and electrical resistivity of the nanocomposite.

Addition of carbon nanotubes to the epoxy made the plates electrically conductive, and the more the MWCNT content, the more electrical conductivity was obtained. However, increasing the concentration of MWCNT also significantly increased the viscosity, and impeded the preparation procedure. Electrical resistivity of MWCNT reinforced epoxy nanocomposites increased with the absorption of water. Because the swelling of the plates automatically increased the distance between nanotubes, and caused the elongation or disconnection of their conductive paths. Electrical resistivity of composites containing less amount of MWCNTs was found to be more sensitive to water absorption. They showed a more pronounced increase in their resistivity due to the limited number of conductive paths between their MWCNTs. In addition, higher aspect ratio of the nanotubes slowed down the water absorption, and helped obtaining better entanglement, more conductive paths, and higher conductivity.

In order to investigate the effect of swelling on the increase of electrical resistivity of the nanocomposite, efforts were made to obtain more pronounced swelling in the material, and study the electrical resistivity behavior. Silicone rubber conductive plates were fabricated and immersed in engine oil. The thickness and the electrical resistivity of these plates exhibited a considerably high increase. It was demonstrated that, the extent of swelling as well as its duration, both strongly

affect the intensity of deagglomeration of carbon nanotubes and the elongation or disconnection of their conductive paths.

Regarding the desorption experiments, it was concluded that similar to absorption, desorption took place faster at higher temperatures. The weight loss curve exhibited a two-stage downward trend including a more rapid linear stage, followed by a non-linear gradual reduction. The residual weight gain in the material was found to be a result of bound water type II existing amongst polymer chains, and was recoverable by elevating the temperature and providing the activation energy to break the hydrogen bonds. Electrical resistivity did not completely recover to its original value, which was assumed to be due to the restructuring of carbon nanotube agglomerations.

4.2 Contributions

This thesis presented a study on the effect of water absorption on the electrical resistivity of MWCNT reinforced epoxy nanocomposites. The contribution of this project can be highlighted as follows:

- The effect of MWCNT concentration on electrical resistivity and water diffusion of MWCNT reinforced epoxy nanocomposites was found experimentally and presented.
- The influence of the aspect ratio of MWCNT on the electrical resistivity and water diffusion of the nanocomposite was investigated and presented.
- The effect of moisture absorption on the electrical resistivity of MWCNT reinforced epoxy nanocomposites was studied and presented.
- A theory was proposed explaining the role of water in elongating or disconnecting nanotube-to-nanotube joints and increasing electrical resistivity.

- Desorption behavior and the recovery of the electrical properties of the nanocomposite were investigated experimentally and presented.

4.3   Recommendations for Future Work

According to this research, some future work is recommended as follows:

- To study the effect of water absorption on the electrical resistivity of the nanocomposite for a wide range of water temperatures

- To study the electrical resistivity behaviour of the nanocomposite in cryogenic temperatures for space technologies and fluid gas container applications

- To study the electrical resistivity of the nanocomposite in other liquids, such as acids and bases, and investigate its corrosion behaviour

- To conduct cycles of sorption-desorption-resorption on the nanocomposite and study the recoverability of their physical and electrical properties

5 References

[1] Hoa, S. V., 2009, *Principles of the Manufacturing of Composite Materials,* Department of Mechanical and Industrial Engineering, Concordia University, Quebec, Canada, Chap. 3.

[2] Starkova, O., Buschhorn, S. T., Mannov, E., Schulte, K., and Aniskevich, A., 2013, "Water Transport in Epoxy/ MWCNT Composites," European Polymer Journal, **49**(13)

[3] May, C. A., and Tanaka, Y., Eds., 1973, *Epoxy Resins Chemistry and Technology*, Marcel Dekker, New York, NY.

[4] Lin, Y.C., Chen, X., 2005, "Moisture Sorption-Desorption-Resorption Characteristics and its Effect on the Mechanical Behaviour of the Epoxy System," Polymer, **46**(5), pp. 11994-12003.

[5] Lin, Y.C., Chen, X., 2005, "Investigation of Moisture Diffusion in Epoxy System: Experiments and Molecular Dynamics Simulation," Chemical Physics Letters, **412**(5), pp. 322-326.

[6] Ardebili, H., Wong, E.H., Pecht, M., 2003, "Hygroscopic Swelling and Sorption Characteristics of Epoxy Molding Compounds Used in Electronic Packaging." Components and Packaging Technologies, IEEE Transactions, **26**.1(3), pp. 206-214.

[7] Preiswerk, E., 1965, *The Recognition of the Bonding Properties of Epoxy Resins*, Technica, Birkhäuser, Chap. 4-5.

[8] Lewis, A. F., and Saxon, R., 1973, *Epoxy-Resin Adhesives*, Industrial Chemicals and Plastic Division American Cyanamid Company, Stamford, CT.

[9] Pillai, S.K., Ray, S.S., 2011, *Epoxy-Based Carbon Nanotubes Reinforced Composites*, InTech. South Africa

[10] Chemical Book, DGEBF, from:

http://www.chemicalbook.com/ProductChemicalPropertiesCB7672361_EN.htm

[11]   Powers, D.A., 2009, "Interaction of Water with Epoxy," Sandia Report SAND2009-4405, Albuquerque, New Mexico.

[12]   Guadagno, L., Vertuccio, L., Sorrentino, A., Raimondo, M., Naddeo, C., Vittoria, V., 2009, "Mechanical and Barrier Properties of Epoxy Resin Filled with Multi-Walled Carbon Nanotubes," Carbon **47**(9), pp. 2419-2430.

[13]   Liang, Z., Gou, J., Zhang, Ch., Wang, B., 2004, "Investigation of Molecular Interactions Between (10, 10) Single-Walled Nanotube and Epon 862 Resin/DETDA Curing Agent Molecules," Materials Science and Engineering, **365**(4), pp. 228-234.

[14]   Mactabi, R., 2011, "In Situ Health Monitoring of Adhesively Bonded Joints during Fatigue Using Carbon Nanotube Network." M.Sc. Thesis, Concordia University, Montreal, Canada.

[15]   Thostenson, E.T., Ren, Z., Chou, T.W., 2001, "Advances in the Science and Technology of Carbon Nanotubes and their Composites: A Review," Composites Science and Technology, **61**(11), pp. 1899-1912.

[16]   Bu, L., Steitz, J., Dinh-Trong, N., Kanoun, O., 2009 "Influence of Processing Parameters on Electrical Properties of Carbon Nanotube Films." Nanotechnology, *9th IEEE Conference,* Chemnitz University of Technology, Chemnitz, Germany.

[17]   Matthias, H., Boehme, B., Sebastian, S., 2009, "CNTs- A Comparable Study of CNT-Filled Adhesives with Common Materials," *Electronic Components and Technology Conference,* Technische Universität Dresden, Dresden, Germany.

[18]   Jiang, H., Zhu, L., Moon, K., Li, Y., Wong, C.P., 2007, "Low Temperature Carbon Nanotube Film Transfer via Conductive Adhesives," *Electronic Components and Technology Conference,* Georgia Institute of Technology, Atlanta, GA.

[19]   Naghashpour, A., 2014, "In-situ Damage and Strain Monitoring of Large Polymer Composite Structures Using Carbon Nanotube Networks," Ph.D. Thesis, Concordia University, Montreal, Canada.

[20]   Prolongo, S.G., Gude, M.R., Urena, A., 2012, "Water Uptake of Epoxy Composites Reinforced with Carbon Nanofillers," Composites Part A: Applied Science and Manufacturing **43**(12), pp. 2169-2175.

[21]   Dutta, S.S., 2008, "Water Absorption and Dielectric Properties of Epoxy Insulation," M.Sc. Thesis, Norwegian University of Science and Technology.

[22]   Ling, Y., Gu, G., Liu, R., Lu, X., 2013 "Investigation of the Humidity-Dependent Conductance of Single-Walled Carbon Nanotube Networks," J. Applied Physics, **113**.2(13), pp. 024312-024312-5.

[23]   Barkoula, N.M., Paipetis, A., Matikas, T., 2009, "Environmental Degradation of Carbon Nanotube-Modified Composite Laminates: A Study of Electrical Resistivity," Mechanics of Composite Materials **45**.1(9), pp. 21-32.

[24]   Rosca, D., Hoa, S.V., 2009, "Highly conductive multiwall carbon nanotube and epoxy composites produced by three-roll milling," Carbon, **47**(2009), pp. 1958-1968 .

[25]   Nanotechnology Now, from http://www.nanotech-now.com

[26]   Wichmann, M.H.G., Sumfleth, J., Gojny, F.H., 2006, "Glass-Fibre-Reinforced Composites with Enhanced Mechanical and Electrical Properties– Benefits and Limitations of a Nanoparticle Modified Matrix," Engineering Fracture Mechanics, **73(**6), pp. 2346-2359.

[27]   Cui, H.W., Kowalczyk, A., Li, D.Sh., Fan, Q., 2013, "High Performance Electrically Conductive Adhesives from Functional Epoxy, Micron Silver Flakes, Micron Silver Spheres

and Acidified Single Wall Carbon Nanotube for Electronic Package," Int. J. Adhesion and Adhesives **44**(13), pp. 220-225.

[28] Yu, S., Tong, M.N., Critchlow, G., 2010, "Use of Carbon Nanotubes Reinforced Epoxy as Adhesives to Join Aluminum Plates," Materials & Design **31**(10), pp. S126-S129.

[29] Li, Y., Wong, C.P., 2006, "Recent Advances of Conductive Adhesives as a Lead-Free Alternative in Electronic Packaging: Materials, Processing, Reliability and Applications," Materials Science and Engineering R, **51**(6), pp. 1-35.

[30] Rosca, I.D., Mactabi, R., Hoa, S.V., 2011, "Influence of the Carbon Nanotube Type, Loading and Chemical Functionalization on the Fatigue Resistance of Aluminum Lap Joints." 26th ICAF Symposium, Concordia University, Montreal, Canada.

[31] Crocombe, A.D., 2008, "Incorporating Environmental Degradation in Closed Form Adhesive Joint Stress Analyses," J. Adhesion, **84**.3(8), pp. 212-230.

[32] Mubashar, A., Ashcroft, I.A., Critchlow, G.W., Crocombe, A.D., 2011, "A Method of Predicting the Stresses in Adhesive Joints after Cyclic Moisture Conditioning." J. Adhesion, **87**.9 (11), pp. 926-950.

[33] Loh, W.K., Crocombe, A.D., Abdel Wahab, M.M., 2004, "Modelling Anomalous Moisture Uptake, Swelling and Thermal Characteristics of a Rubber Toughened Epoxy Adhesive." Int. J. Adhesion and Adhesives **25**(5), pp. 1-12.

[34] Zhou, J., Lucas, J.P., 1994, "The Effects of a Water Environment on Anomalous Absorption Behaviour in Graphite/Epoxy Composites," Composites Science and Technology, **53**(95), pp. 57-64.

[35]   Springer, G. S., 1981, *Environmental Effects on Composite Materials*, Department of Mechanical Engineering & Applied Mechanics, The University of Michigan Ann Arbor, Michigan, Chap.

[36]   Glaskova, T.I., Guedes, R.M., Morais, J.J., Aniskevich, A.N., "A Comparative Analysis of Moisture Transport Models Applied to an Epoxy Binder", Institute of Polymer Mechanics, University of Latvia, Riga, Latvia

[37]   Popineau, S., Rondeau-Mouro, C., 2005, "Free/Bound Water Absorption in an Epoxy Adhesive," Polymer, **46(**5), pp. 10733-10740.

[38]   Crank, J., 1975, *The Mathematics of Diffusion*, Oxford, Clarendon press, Vol. 2., No. 3.

[39]   Wu, Ch., Xu, W., 2007, "Atomistic Simulation Study of Absorbed Water Influence on Structure and Properties of Cross-linked Epoxy Resin," Polymer, **48**(7), pp. 5440-5448.

[40]   Zhou, J., Lucas, J.P., 1998, "Hygrothermal Effects of Epoxy Resin. Part I: The Nature of Water in Epoxy," Polymer, **40**(99), pp. 5505-5512

[41]   Zhou, J., Lucas, J.P., 1998, "Hygrothermal Effects of Epoxy Resin. Part II: Variations of Glass Transition Temperature," Polymer, **40**(99), pp. 5513-5522.

[42]   Kwei, T.K., "Strength of Epoxy Polymers. I. Effect of Chemical Structure and Environmental Conditions," J. Applied Polymer Science **10**(66), pp. 1647-1655.

[43]   Beuche, F., 1965, *Physical Properties of Polymers*, Interscience, New York, NY.

[44]   Xiao, G.Z., Shanahan, M.E.R., 1997, "Swelling of DGEBA/DDA Epoxy Resin During Hygrothermal Aging," Polymer, **39**(97), pp. 3253-3260.

[45]   Wikipedia, Van der Pauw Method, from:

    http://en.wikipedia.org/wiki/Van_der_Pauw_method

[46]   Van der Pauw, L. J., "A Method of Measuring the Resistivity and Hall Coefficient on Lamellae of Arbitrary Shape," Philips technical review, **20**.8(1958), pp. 220-224.

[47]   Hexion,   2005,   EPON   862   MSDS,   from http://www.hexion.com/Products/TechnicalDataSheet.aspx?id=3950

[48]   Harley, S.J., Glascoe, E.A., Maxwell, R.S., 2012, "Thermodynamic Study on Dynamic Water Vapor Sorption in Sylgard-184," J. Physical Chemistry B, **116**(12), pp. 14183-14190.

[49]   Abd-El Salam, M.H., El-Gamal, S., Abd-El Maqsoud, D.M., Mohsen, M., 2013, "Correlation of Electrical and Swelling Properties with Nano Free-Volume Structure of Conductive Silicone Rubber Composites," Polymer Composites, **34(**13), pp. 2105-2115.

[50]   Krayden, Sylgard 184, from http://krayden.com/sylgard-184/